Editorial Manager(tm) for Ocean Dynamics
Manuscript Draft

Manuscript Number: ODYN-D-10-00150R1

Title: A model study of tidal distributions in the Celtic and Irish Sea regions determined with finite volume and finite element models.

Article Type: Special Issue - Jonsmod 2010

Keywords: unstructured girds; modelling; tides; Irish Sea

Corresponding Author: Jiuxing Xing, Ph.D.

Corresponding Author's Institution:

First Author: Alan Davies

Order of Authors: Alan Davies;Jiuxing Xing, Ph.D.

Abstract: An unstructured mesh tidal model of the west coast of Britain, covering the Celtic Sea and Irish Sea is used to compare tidal distributions computed with finite element (F.E.) and finite volume (F.V.) models. Both models cover an identical region, use the same mesh, and have topography and tidal boundary forcing from a finite difference model that can reproduce the tides in the region. By this means solutions from both models can be compared without any bias towards one model or another. Two dimensional calculations show that for a given friction coefficient there is more damping in the F.V. model than the F.E. model. As bottom friction coefficient is reduced the two models show comparable changes in tidal distributions. In terms of mesh resolution, calculations show that for the M2 tide the mesh is sufficiently fine to yield an accurate solution over the whole domain. However in terms of higher harmonics of the tide, in particular the M6 component, its small scale variability in near shore regions which is comparable to the mesh of the model, suggests that the mesh resolution is insufficient in the near coastal regions. Even with a finer mesh in these areas, without detailed bottom topography and a spatial varying friction depending on bed types and bed forms, which is not available, model skill would probably not be improved. In addition in the near shore region, as shown in the literature, the solution is sensitive to the form of the wetting/drying algorithm used in the model. Calculations with a three dimensional version of the F.V. model show that for a given value of k, damping is reduced compared to the two dimensional version due to the differences in bed stress formulation, with the three dimensional model yielding an accurate tidal distribution over the region.

Detailed Response to Reviewer's comments on paper D-10-150 "A model study of tidal distributions in the Celtic...." by Davies et al.

General Response

Comments such as "this paper is very interesting, clear and well organised" and "merits publication... minor corrections" (Ref 1) are much appreciated. In addition that Ref 2, finds the objective of the paper "interesting" is good to read.

In revising the paper we have taken account of both sets of reviewers comments.

Detailed Response to Ref 1.

(1) Tables of M4/M2 amplitude ratio and where possible M6/M2 ratio for sites where M6 exceeds 5cm, have now been added and discussed.
(2) P4, L35, FVCOM, spelled out.
(3) P5, L33, typing corrected.
(4) Where possible annotation on cotidal charts improved.

Detailed Response to Ref 2.

(1) Description of models slightly enhanced. As a detailed description is given in published papers, these are cited, as we do not wish to repeat information. In addition since a functional form of the solution is given over each finite element or finite volume this can be used to interpolate solutions (e.g. water elevations) to any location. This point made in text.
(2) It is made clear that the staircase representation of the coastline only relates to a certain class of finite difference model.
(3) The k-0.003 calculations are mentioned "early on".
(4) Possibility of lack of mesh resolution influencing solution of higher harmonics is discussed in context of the fact that this could also be influenced by "wetting and drying". Additional references added.
(5) Abstract rephrased to suggest this, rather than claim that it has been shown. Similar in text.
(6) Elaborated to show that in the near short region the amplitude of the higher harmonics changes very rapidly from one mesh element to another. A sure sign of a lack of spatial convergence. The confusion between temporal convergence, where iteration ensures that a converged solution does occur and spatial convergence is now clarified.
(7) The realistic nature of these coefficients is confirmed by reference to published observed bottom friction coefficients that occur in the region.

Summary

Paper revised taking account of all reviewers comments. Our thanks to reviewers and editor for comments and time taken to review the paper.

A model study of tidal distributions in the Celtic and Irish Sea regions determined with finite volume and finite element models.

by

Alan M Davies, Jiuxing Xing and John Eric Jones

National Oceanography Centre

6 Brownlow Street

Liverpool L3 5DA

England, U.K.

Abstract

An unstructured mesh tidal model of the west coast of Britain, covering the Celtic Sea and Irish Sea is used to compare tidal distributions computed with finite element (F.E.) and finite volume (F.V.) models. Both models cover an identical region, use the same mesh, and have topography and tidal boundary forcing from a finite difference model that can reproduce the tides in the region. By this means solutions from both models can be compared without any bias towards one model or another. Two dimensional calculations show that for a given friction coefficient there is more damping in the F.V. model than the F.E. model. As bottom friction coefficient is reduced the two models show comparable changes in tidal distributions. In terms of mesh resolution, calculations show that for the M_2 tide the mesh is sufficiently fine to yield an accurate solution over the whole domain. However in terms of higher harmonics of the tide, in particular the M_6 component, its small scale variability in near shore regions which is comparable to the mesh of the model, suggests that the mesh resolution is insufficient in the near coastal regions. Even with a finer mesh in these areas, without detailed bottom topography and a spatial varying friction depending on bed types and bed forms, which is not available, model skill would probably not be improved. In addition in the near shore region, as shown in the literature, the solution is sensitive to the form of the wetting/drying algorithm used in the model. Calculations with a three dimensional version of the F.V. model show that for a given value of k, damping is reduced compared to the two dimensional version due to the differences in bed stress formulation, with the three dimensional model yielding an accurate tidal distribution over the region.

1. Introduction

To date the most common approach used in oceanography to model tidal distributions in a region has been the application of uniform grid finite difference methods. Initial calculations were restricted by lack of computational power to coarse grid limited area models, such as the west coast of Britain model of Davies and Jones (1992) (hereafter DJ92) which had a grid resolution of the order of 7km. Subsequently the domain of such models was expanded to the whole of the Northwest European Continental Shelf (Kwong et al., 1997, Davies and Kwong 2000), although the grid resolution remained coarse at the order of 10km. With such coarse grids it was not possible to accurately include the near shore regions where "wetting and drying" occurred over a tidal cycle and important non-linear processes lead to the generation of higher harmonics of the tide. To overcome these difficulties higher resolution limited area models were developed such as the 1km eastern Irish Sea model of Jones and Davies (1996)(hereafter JD96). Although in the eastern Irish Sea this model could resolve the near shore region where "wetting and drying" occurred and non-linear effects gave rise to higher harmonics of the tide, the limited geographical extent of the model meant that these higher harmonics had to be specified along the open boundaries of the model. Hence the distribution of these higher harmonics was determined by both model dynamics and the open boundary condition. Consequently the ability of the model to generate higher harmonics could not be tested independently of the open boundary conditions. An alternative approach is to nest a higher resolution finite difference model within one of coarser resolution. However, the false reflection at the interface between the models of waves that can be resolved on the fine grid but not the coarse grid, is a major deficiency of this approach. In addition as shown by Aldridge and Davies (1993), the "stair-case" nature of the coastal boundary in the majority of conventional finite difference models (the exception being those that use a boundary fitted coordinate) produced "spurious solutions" in a near coastal boundary layer of the order of three to four grid boxes wide.

An alternative approach to the application of finite differences is to use an unstructured mesh, and solve the resulting equations by applying the finite element method. The application of this technique in oceanography has recently been reviewed by Jones (2002), Walters (2005), and Greenberg et al.

(2005, 2007), and consequently details will not be presented here. Some recent applications to tidal problems are given in e.g. Foreman et al. (1993, 1995), Fortunato et al. (1997), Ip et al. (1998), Legrand et al. (2006, 2007), Levasseur (2007), Lynch et al. (1993, 2004) and Walters (1992). A comparison of the performance of finite difference and finite element models for reproducing the M_2 tide and its higher harmonics in the English Channel was performed by Werner (1995). However, as the model domain was limited higher harmonics were included in the open boundary condition. Also there were no significant "wetting and drying" areas in the region which as shown by Greenberg et al. (2005), Jones et al. (2008), Chen et al. (2008) and Karna et al. (2011) significantly influence tidal distributions in shallow regions. In addition because of the limited domain of the model the M_2 tidal solution was constrained by the open boundary. Consequently a detailed comparison of the performance of finite difference and finite element solutions in such conditions was not possible.

In this paper the tidal distribution over a much larger domain is considered, namely the west coast of Britain which was first examined by DJ92 using a finite difference approach. In this case the model open boundaries are well removed (Fig 1a) from the region of interest, namely the eastern Irish Sea (Fig 1b) where "wetting and drying" occurs and higher harmonics are generated. Consequently only the M_2 tide along the open boundary is used to force the model, and higher harmonics which are important in the eastern Irish Sea are generated by the model. By this means it is possible to compare the performance of a finite volume (F.V.) model, based on FVCOM (Finite Volume Coastal Ocean Model) and a finite element (F.E.) model namely TELEMAC in a shallow nearshore region, namely the eastern Irish Sea, which is well removed from the region of boundary forcing (Fig 1a). In addition by using an identical domain, boundary forcing and topography to that used earlier by DJ92 in a finite difference model, the tidal solution is not biased towards either the F.V. or the F.E. approach.

The objective of the paper is to compare tidal solutions computed with a F.V. model based on FVCOM (Chen et al 2003, 2007, Huang et al 2008), with those derived from a F.E. model namely TELEMAC (e.g. Hervouet, 2002, Jones and Davies 2005, 2007, 2010, Malcherek 2000, Nicolle and Karpytchev 2007), under identical conditions of boundary forcing and bottom topography. The form of the hydrodynamic equations and brief details of the models, with references to the literature for more extensive technical details is presented in the next section. Tidal solutions and comparisons with

observations are presented subsequently, with a conclusions section summarising the main findings from the study.

2. Hydrodynamic equations and model formulations.

As the primary aim of the paper is a comparison of tidal elevations computed with finite volume and finite element models, then the majority of the calculations were performed with two dimensional vertically integrated models. To be consistent with earlier finite difference calculations, the bottom friction coefficient k was initially set at a constant value of k=0.003, although subsequently this was reduced to k=0.0025 (Table 1). However as shown by Aldridge and Davies (1993), and Davies and Lawrence (1995)(see their Fig 2) bed types and bed forms vary significantly over the eastern Irish Sea, and to examine the sensitivity to bottom friction coefficient, the F.V. model was also run with k set at half this value, namely k=0.00125. This range of friction coefficients is physically justified and corresponds to the range of bed types found in the Irish Sea that vary from gravel (high k value) to mud (low k value) (see Davies and Lawrence 1995). In addition to see to what extent tidal elevation is sensitive to three dimensional effects, the F.V. model was run in three dimensions with 21 sigma levels in the vertical. In this case k was determined from

$$k=\max\left\{0.0025, \left[\frac{K}{\ln(Z_r/Z_0)}\right]^2\right\} \qquad (1)$$

where K= Von Karman's constant with Z_r= reference height and Z_0 bed roughness. As both models are fully non linear (see Hervouet, 2002, Malcherek, 2000, Jones and Davies 2010, for details of TELEMAC, and Chen et al 2003, 2007 for details of FVCOM), and contain "wetting and drying" (see for example Chen et al (2008) and Karna et al (2011) for a detailed discussion of "wetting and drying" and references to algorithms for implement it), which occurs when the total water depth falls below 0.05m, then they contain all the necessary physics for generating higher harmonics of the tide in shallow water. As the physics of higher harmonic generation is given in Davies 1986, Filloux and Snyder 1979, Heaps 1978, Inoue and Garret 2007, LeProvost 1991, Walters and Werner 1991, Jones and Davies 2010, it will not be discussed here. In all calculations (Table 1), solutions were generated from initial conditions of zero elevation and motion at t=0, by integrating over seven tidal cycles and harmonically analysing the final cycle for the M_2, M_4 and M_6 tides. At closed boundaries, the normal

component of velocity was zero, and the horizontal gradient normal to the coast of alongshore velocity was set to zero. This gave a perfect lateral slip condition.

The model domain, water depths and tidal open boundary condition were the same in all calculations and were taken from the finite difference model of DJ92. The unstructured mesh used in the calculations (Grid G3AX, Fig 2) was generated using a mesh refinement based on water depth such that the ratio between element size and $(gh)^{½}$ was constant, with g acceleration due to gravity and h water depth. This gave a maximum element size of order 5km in deep water and 0.5km for near shore elements.

3. Numerical solution using the F.E. and F.V. models.

As the TELEMAC finite element code has been used extensively and is well documented (see for example Jones and Davies (2010) and references therein) details will not be presented here. In addition, as details of the F.V. code formulation are given in Chen et al (2003, 2007), they will not be repeated here. Both models use time integration methods that ensure an accurate converged solution in the time domain. However accuracy in the spatial domain is determined by the specified mesh resolution which is fixed and does not vary with time. Consequently although the mesh may be sufficiently fine to represent the large scale spatial variability of the M_2 tide it may be insufficient to accurately resolve short wavelength higher harmonics such as M_6 which are generated in coastal regions (see later discussion). An extensive comparison with observations at a number of coastal and offshore positions (see Fig 1c for locations) for the M_2, M_4 and M_6 tidal elevation amplitude and phase in the eastern Irish Sea is given in Tables 2, 3 and 4. By applying the functional form of the elements used in both approaches, values can be interpolated from element nodes where they are computed to any spatial location in order to compare with observations (see Chen et al (2003) and references in Jones and Davies (2010) for more details). The accuracy of the two models for a range of friction coefficients is presented here in terms of the comparisons with observations given in these tables.

3.1 The F.E. model with k=0.003 (Calc 1 (F.E.)).

In an initial calculation (Table 1, Calc 1 (F.E.)), tides were computed using the F.E. model. As a detailed discussion of cotidal distributions in the Irish and Celtic Seas is given elsewhere (eg. DJ96,

Davies (1986), George (1980), Robinson (1979), Jones (1983)) only the major features are presented here, where the main focus is an intercomparison of F.E. and F.V. solutions and the influence of bottom friction upon these. The M_2 cotidal chart derived from the F.E. model (Fig 3a), shows a degenerate amphidromic point off the south-east coast of Ireland, with tidal amplitudes increasing rapidly in the shallow water of the eastern Irish Sea, and within the Bristol Channel. The overall distribution of the tidal amplitude and phase in the Irish and Celtic Seas is in good agreement with observations, and Irish Sea cotidal charts derived by Robinson (1979) based on observations. In the northern part of the model, namely within the North Channel of the Irish Sea, the rapidly changing tidal distribution associated with a second degenerate amphidromic point (Fig 3a), is reproduced with a comparable accuracy to that found in limited area high-resolution models of this region (Davies et al. 2001). A detailed comparison with measurements at coastal and off-shore gauges in the eastern Irish Sea (Table 2) shows that on average there is good agreement between model and observations, although at some locations computed amplitude and phase are overestimated by 10cm and 5°.

The largest errors between model and observations occur at locations that are adjacent to large regions of shallow water, e.g. Hilbre, Conwy, the three tide gauges Y,Z and AA in close proximity to each other and located near Barrow (Fig 1c), and at Morecambe (BB) and Fleetwood (CC). As shown by Jones et al (2009) although the mesh has high resolution in these areas, namely a mesh length of order 500m, this is not sufficient to accurately resolve the M_2 tidal variations that occur over very short distances (less than 500m) in these coastal regions. This lack of resolution suggests that in order to improve the accuracy of the M_2 tide in these regions, a higher mesh resolution is required. However without a more detailed and accurate set of bathymetry and a spatially varying friction coefficient reflecting bed types and bed forms, any improvement could be small. In addition the form of the "wetting/drying" algorithm will also influence the solution in the near shore region (see for example the discussion in Karna et al. (2011). However, since the primary aim here is to examine differences in the F.E. and F.V. calculations, using identical meshes, boundary forcing and water depth, this lack of high resolution in near coastal regions is not significant.

The M_4 cotidal chart (Fig 3b), shows the M_4 tidal amplitude increasing over the Celtic Sea from zero at the open boundary to a maximum of 10cm in the southern part of the Irish Sea. Subsequently the M_4 amplitude decreases to a minimum to the west of the Isle of Man (Fig 3b). A rapid increase in the shallow coastal regions of the eastern Irish Sea is evident. This spatial distribution is found in observations and shelf wide finite difference models (Davies and Kwong 2000). Comparisons with a high resolution (1km) finite difference limited area eastern Irish Sea model (JD96), showed that the M_4 distribution computed with the present model was of comparable accuracy. The high accuracy obtained by JD96, was in part due to the specification of the M_4 tide along the open boundary of that model, which only covered the eastern Irish Sea. The fact that the present model with no M_4 input and covering a large area can reproduce this M_4 distribution suggests that the present model contains the necessary physics to reproduce the M_4 tide in the region. As for the M_2 tide, it is evident from Table 3, that at a number of coastal locations there are significant errors in the M_4 tide computed with the model. This is in part, as discussed for the M_2 tide, due to a lack of mesh resolution. In addition in some shallow coastal regions (e.g. Barrow RI) there is extensive "wetting and drying" which removes energy from the M_2 tide, the amplitude of which is decreased compared to observations due to excessive energy going into the M_4 tide arising from the "wetting and drying". With a finer mesh and more accurate depth distribution the region of "wetting and drying" would change, with an associated change in energy transfer from M_2 to M_4. In a detailed study of tide-surge interaction involving the spatial distribution of non-linear terms in coastal regions, Xing et al (2010) showed that on the present mesh there was significant spatial variability in coastal regions from one node to another.

A rapid increase in M_6 tidal amplitude (Fig 3c) occurs in shallow water in the Liverpool Bay region and in the Cumbrian coastal area as water is particularly shallow here, and there is significant "wetting and drying" which leads to a local increase in M_6. Point by point comparisons (Table 4) show that at a number of shallow water locations e.g. Barrow, Birkenhead, Hilbre, Barrow HP, the computed amplitude exceeds the observed. In these regions there is very rapid spatial variability from one node to another, suggesting that the model mesh is too coarse. In addition the depth distribution

used in the model is not sufficiently accurate to resolve local near coastal variations in water depth that determine the exact location of "wetting and drying" regions and the detailed distribution of the M_6 tide. A close examination of tidal distributions in particular the higher harmonics namely M_4 and M_6 in regions such as the Solway estuary and Morecambe Bay (Fig 3b(ii) and 3c(ii)) clearly shows significant small scale variability, suggesting that more detailed coastal resolution is required, with an associated enhancement of the mesh, in order to resolve this variability. However, as shown by Aldridge and Davies (1993) and Davies and Lawrence (1995) there is significant spatial variation in bed types and bed forms over the Irish Sea, giving rise to spatial variability in the bottom friction coefficient that must be taken into account in any detailed simulation of tides or surges in near shore regions (e.g. Nicolle and Karpytchev 2007). Since, as stated previously the objective of the present paper is a comparison of F.E. and F.V. models the use of a constant friction coefficient is justified. However, the sensitivity of the various solutions to changes in the value of k will also be considered later.

3.2 The F.V. model with k=0.003 (Calc 1 (F.V.))

In a subsequent calculation (Calc 1 (F.V.)) the tidal distribution over the region was computed with the F.V. model and k=0.003. The computed M_2, M_4 and M_6 cotidal charts show similar distributions to those found with the F.E. model. Although there is no significant difference in the distribution of co-amplitude and co-phase lines in the region of the northern and southern boundaries the location of the amphidromic point in the North Channel is slightly different to that found in the F.E. model. In addition the position of the degenerate amphidromic point off the east coast of Ireland has moved farther north. This has the effect of decreasing M_2 amplitudes in the region to the north and south of the Isle of Man, namely the western boundary of the eastern Irish Sea by the order of over 40cm (see difference plots Fig 4a(i)(ii)). A consequence of this is that tidal amplitudes in the shallow coastal region of eastern Irish Sea computed with the F.V. model are of the order of 35cm to 40cm lower than those computed with the F.E. model (see difference plots Fig 4a(i)(ii)) and found in observations (Table 2). This suggests that in shallow coastal regions the M_2 tide computed with the

F.V. model is more heavily damped than that computed with the F.E. model, although there is little difference in phase.

For the M_4 component, its distribution in the eastern Irish Sea (see difference plots Fig 4b (i)(ii)) is comparable to that found with the F.E. model, although its magnitude at coastal gauges (Table 3) is reduced compared to the F.E. model, due to the reduction in the M_2 tide in the F.V. model compared to the F.E. model. Although its magnitude is reduced, it shows a similar spatial distribution of high and low values at coastal ports, as found in the observations and the F.E. solution. For example (Table 3), computed high (over 25cm) M_4 amplitudes at Barrow, Birkenhead, Hilbre, Liverpool, New Brighton, Creetown, Conwy, Barrow (RI, HP), Morecambe, Fleetwood, with computed low (under 10cm) at Douglas, Wylfa Head, Amlwch and STD Irish Sea occur in both solutions (Table 3). This suggests comparable M_4 amplitude distributions, although quantitatively those computed with the F.V. model are below those computed with the F.E. model. In terms of phase differences between the solutions, at coastal gauges there are significant differences, and no clear pattern in the distribution of these differences. However, at off shore gauges (Q, R, S, T, U, V) there are only slight (on average of order 4°) differences in the phase computed with the two models. This suggests that tidal distributions at off shore gauges can be accurately resolved, whereas at coastal gauges, further resolution is required in order for the small scale tidal variations to be resolved. However, the significant difference in the M_2 tidal amplitudes in shallow regions between the F.E. and F.V models does suggest differences in their damping characteristics.

For the M_6 tide, the F.V. model shows a similar spatial distribution to that found with the F.E. model, namely a decrease in amplitude from the region to the north-east of the Isle of Man, to a minimum to the east of the Isle of Man, and a rapid increase moving south of this and into Liverpool Bay. However, despite this agreement, difference plots (Fig 4c (i)(ii)) and Table 4, show on average a reduced M_6 amplitude computed with the F.V. model compared to the F.E. model. This is certainly due to the differences found in the M_2 tidal amplitude in the eastern Irish Sea region computed with these models. As with the F.E. model there is significant spatial variability in the phase computed with the two models in coastal areas, although more consistent phases are found at offshore gauges.

This again emphasises the need to refine the mesh in shallow regions in order to accurately resolve the higher harmonics.

4. Influence of bottom friction upon tidal distributions.

In the previous section it was evident from Tables 2,3 and 4, that the F.E. model with k=0.0030 could accurately reproduce the M_2 tide in the region. However, with this value of friction coefficient the F.V. model had a tendency to underestimate the M_2 tide which had consequences for the other tidal constituents. In this series of calculations k is reduced to 0.0025 to see how this influences the tidal solutions.

4.1 The F.E. model with k=0.0025 (Calc 2 (F.E.))

Although the distribution of the co-amplitude and co-phase lines (not shown) computed with the F.E. model with k=0.0025 is comparable to that found previously (Fig 3a (i)(ii)), the effect of reducing the bottom friction coefficient is to increase the M_2 amplitude above that found in the observations (see Table 2). This arises because of a decrease in energy dissipation through bottom friction. It is evident from Table 2, that the phase of the tide is not appreciably influenced. This increase in M_2 tidal amplitude is accompanied by an increase in amplitude of the M_4 and M_6 tide in the eastern Irish Sea (see Tables 3 and 4).

4.2 The F.V. model with k=0.0025 (Calc 2 (F.V.)).

In the case of the F.V. model, as with the F.E. model reducing k leads to an increase in tidal amplitude (see Tables 2,3,4). This produces a change in the location of the tidal amphidrome in the North Channel and off the east coast of Ireland, and an increase in the M_2 amplitude computed with the F.V. model. However, it is evident compare Figs 5a (i)(ii) and Fig 3a(i)(ii) that the F.V. model even with k reduced to 0.0025, still underpredicts that computed with the F.E. model (k=0.003) and found in observations (Calc 2, F.V.)(Tables 2,3,4). It is evident from Table 2, that at offshore gauges (Q,R,S,T,U,V) the M_2 tidal amplitude computed with the F.E. model (k=0.0030) tended to be overestimated by the order of 15cm. In the calculation with the F.V. model (k=0.0025)Calc 2(F.V.)) the amplitude of the M_2 tide is underestimated by a comparable amount, even though bottom friction is substantially less. In the case of the F.E. model (k=0.0030)(Calc1(F.E.)) the fact that the model

overestimates the tide at off shore gauges by 15cm, appears to be corrected for by enhanced dissipation in shallow water resulting in an accurate simulation of M_2 tidal amplitude at coastal locations such as Birkenhead, Heysham and Liverpool (G.D.) (Table 2). On the other hand for the F.V. model (Calc 2(F.V.)) (k=0.0025), the error of order -15cm, at off shore gauges, leads to an enhanced error at Birkenhead (-38cm), Heysham (-26cm), and Liverpool G.D. (-33cm) (Table 2, Calc 2 (F.V.)). This suggests that the F.V. code over-damps the M_2 tide in both deep and shallow water. In the case of the F.E. code, there is too little damping in deep water, with the overdamping in shallow water, to a certain extent correcting for it.

These differences in the M_2 solution computed with the F.E. and F.V. model are reflected in the M_4 and M_6 solutions in Tables 3 and 4, and eastern Irish Sea co-tidal charts (Figs 5 (b) and (c)). In terms of the M_4 tide it is evident from Table 3 (comparison of Calc 1 (F.E.) (k=0.0030) and Calc 2 (F.V.) (k=0.0025)) that the reduced M_2 tidal elevation in the F.V. calculation leads on average to a reduction in the M_4 tidal amplitude compared to the F.E. calculation, producing better agreement with observations at a number of ports (e.g. Hilbre, Liverpool, New Brighton). In terms of phase differences between the two solutions, on average these are of the order of 10°. In addition, comparison of co-tidal charts (Fig 3b(ii)(F.E. k=0.003), and Fig 5b (F.V. k=0.0025)) shows a reduced M_4 in the eastern Irish sea with the F.V. model even when k=0.0025.

For the M_6 tide point values (Table 4) and comparison of Figs 3c(ii) and 5c show that the amplitude computed with the F.V. model (Calc 2 (F.V.), k=0.0025) is smaller than that computed with the F.E. model (Calc 1 (F.E.), k=0.0030), reflecting differences in the M_2 solution between the two models. As discussed previously in connection with Calc 1, F.E. and F.V. intercomparisons, there is no clear pattern in the phase difference between the two solutions. These comparisons do however clearly show that even when the bottom friction coefficient is reduced in the F.V. model below that used in the F.E. model, the computed tidal amplitude is below the observed. This suggests that there is more damping in the F.V. model than the F.E. model.

In order to further examine the differences between observations and the various model results it is valuable to compute (Tables 5 and 6) the ratio of the amplitudes of the M_4 and M_6 tides to the M_2 tide for locations where the amplitude exceeds 5cm. This value was chosen because amplitudes below 5cm may be more prone to significant errors. Such a comparison is useful in that it indicates the extent to which energy is transferred from the fundamental to its higher harmonics.

Comparing results computed with k=0.0030 (Tables 5 and 6) for the F.E. and F.V. models (Calcs 1(F.E.) and 1(F.V.) it is evident that on average, the M_4/M_2 ratio, computed with the F.V. model is less than that determined with the F.E. model, reflecting the reduced M_2 amplitude computed with the F.V. compared to F.E. model. However, in general both models show a similar variation in this ratio from one port to another, reflecting that they both produce a significant M_4 tide in regions where observations show a large M_4 tide.

Although, as shown previously decreasing the value of bottom friction (Calcs 2 (F.E.) and 2(F.V.)) leads to an increase in M_2 amplitude in both models, the ratio of M_4 to M_2 on average decreases slightly due to the fact that the M_4 amplitude is not appreciably influenced by this decrease in friction (Table 3).

For the M_6 tidal constituent computed with k=0.003 (Calcs 1) both models show similar M_6 to M_2 ratios (Table 6), with the F.V. model on average having a lower value due to the reduced M_2 tide computed with this model. When the bottom friction coefficient is reduced (Calcs2) both models show that on average this ratio increases slightly due to the increase in the M_2 tide giving a larger M_6 tide as more energy is transferred to it.

These similar spatial variations in M_4 and M_6 ratios, and changes with bottom friction suggest that both models exhibit a similar conversion of M_2 energy into its higher harmonics, despite some differences in M_2 amplitude.

4.3. The F.V. model with k=0.00125 (Calc 3 (F.V.))

Halving the value of bottom friction in the F.V. model to k=0.00125, (Calc (3)(F.V.)) causes the amphidromic point off the east coast of Ireland to move off shore and farther to the north (Fig 6a(i)). This is consistent with tidal calculations of Davies and Aldridge (1993), who found that as bottom friction in a three dimensional spectral model of the Irish Sea was reduced this amphidromic point had a tendency to move to the east. The effect of this change in position of the amphidrome is to increase the tidal amplitude in the region to the north and south of the Isle of Man by the order of 20cm (Fig 6a (i)(ii)) compared to the F.V. solution with k=0.0025 (Fig 5a(ii)). This enhanced coastal amplitudes to a similar extent, as can be seen from Table 2 (compare Calc 2 (F.V.)(k=0.0025)) and Calc 3 (F.V.)(k=0.00125). The effect of this change in k, upon phase was small (of the order of 3°). Despite this reduction in k, M_2 amplitude at coastal gauges remained below those computed with the F.E. model with k=0.003, as shown in Table 2 (compare Calcs 1(F.E.) and 3 (F.V.)).

This reduction in k did not appreciably influence the M_4 tide in the eastern Irish Sea computed with the F.V. model (k=0.00125) compared with the earlier F.V. solution (k=0.0025)(see Table 3 and Fig 6b compared with 5b). In addition, away from the near shore region the F.V. model M_4 tidal distribution computed with k=0.00125 was comparable to that found in the F.E. model with k=0.003 (compare Fig 3b(ii) and 6b) although in the near shore region there were some differences. Also there were some changes in phase at coastal gauges which on average were reduced by about 20°, although this varied from location to location. As found previously, the F.V. model tended to underestimate the M_4 amplitude compared to the F.E. model (k=0.0030) in near shore regions (compare Figs 3b(ii) and 6b). For the M_6 component of the tide the distribution in the eastern Irish Sea (Fig 6c) was appreciably different to that found with the F.V. model (k=0.0025) (Fig 5c) and that computed with the F.E. model (k=0.003)(Fig 3c(ii). In essence M_6 tidal amplitudes in the northern part of the region had increased with a slight decrease in the Liverpool Bay area and off the north coast of Wales. Since the quadratic friction term is a major source of the M_6 tide, it is evident that the value of k can influence its distribution in the eastern Irish Sea, and at coastal locations (compare Calcs 2 (F.V.) and Calc 3 (F.V.) in Table 4).

This series of calculations clearly shows that even when k is reduced in the F.V. calculation, to such a degree that the amphidromic point off the east coast of Ireland moves to the east, the model still slightly underpredicts the M_2 tide in the eastern Irish Sea compared to the observed. In addition this significant reduction in k, changes the M_6 tidal distribution in the region. Since bottom friction plays an important role in M_6 generation, and to examine to what extent three dimensional effects influence tidal elevations, a three dimensional F.V. calculation was performed.

5. Three dimensional F.V. model with minimum k=0.0025 (Calc 4(F.V.)).

In order to determine three dimensional effects the F.V. model was run with 21 sigma levels and bottom friction formulation given by equation (1). Consequently over the deeper water region (h>60m) k=0.0025, however in shallow water where the value of Z_r is small, and the bottom boundary layer can be resolved, then k is determined by the values of Z_r and Z_0 (taken as 0.001m), and is larger than 0.0025.

The computed M_2 co-tidal chart determined with the three dimensional model, (Fig 7a(i)(ii)) shows a similar distribution to that determined with the F.V. model with k=0.00125. Although the bottom friction coefficient in the three dimensional model has a minimum value of 0.0025, and is higher in shallow water, the bed stress is determined by the bottom current rather than the depth mean current. Consequently the bed stress will be smaller than in a two dimensional model with an equivalent value of k. This is the reason why the cotidal chart computed with the three dimensional model corresponds more closely to that computed with the two dimensional model with k=0.00125 than k=0.0025. Similarly in the eastern Irish Sea the position of the 220cm co-amplitude lines (Fig 7a(ii)) occur at similar locations to those found in the two dimensional F.V. model (k=0.00125). However, the location of the 240cm co-amplitude line is slightly different, with the 310° co-phase line showing the effect of enhanced bottom friction in the three dimensional model in the eastern Irish Sea.

A port by port comparison (Table 2, Calc 3 (F.V.) and Calc 4 (F.V., 3D)) reveals a reduction of about 3cm and small phase change of a few degrees between the two solutions, with the three

dimensional F.V. model also underpredicting the tide compared to the F.E. model (k=0.003) and observations, despite the reduced friction coefficient over the majority of the region.

For the M_4 tide in the eastern Irish Sea (Fig 7b), in the region of the Isle of Man there are no appreciable differences in the 2D and 3D solutions (compare Fig 6b and 8b). However, in the coastal region of the eastern Irish Sea, the M_4 amplitude in the 3D model exceeds that found in the 2D model and this is clearly seen in Table 3 (compare Calcs 3 and 4). In particular at ports such as Birkenhead, Hilbre, Liverpool and New Brighton, the M_4 tidal amplitude from the 3D model exceeds that from the 2D model by about 3cm. In terms of phase there are differences at these ports of the order of 15° to 20°.

For the M_6 tide in the eastern Irish Sea, it is evident from a comparison of Figs 7c and 6c that its amplitude had been reduced in the northern part of the region from that found in the 2D model. This reduction in amplitude with an associated change in phase is evident in the coastal gauge comparisons (Table 4, Calcs 3 and 4).

This comparison between 2D and 3D versions of the F.V. model and the F.E. model, clearly shows that even when calculations are performed with the 3D model with a reduced value of k compared to the F.E. model, the M_2 tidal amplitude is underestimated. This confirms the results found with the earlier 2D versions of the models, namely that the damping in the F.V. model is significantly larger than that in the F.E. model.

6. Concluding Remarks

An intercomparison of M_2 tidal distributions and its higher harmonics over the Celtic and Irish Sea regions has been performed using a F.E. and F.V. model. The same irregular mesh, bottom topography and M_2 tidal open boundary forcing was used in all calculations. By this means differences in F.E. and F.V. solutions could be attributed to differences in model formulation. By using the same model domain, topography and open boundary forcing as that employed in an accurate tidal finite difference model, there was no inherent bias towards the F.E. or F.V. models. Also the

influence of changing bottom friction coefficient in each model could be determined. In addition in the case of the F.V. model comparisons between 2D and 3D models were made.

Comparisons with a detailed set of M_2 tidal elevation amplitudes in the eastern Irish Sea, showed that an accurate solution was obtained with the F.E. model with k=0.003. In the case of the F.V. model with the same k value, the solution yields M_2 amplitudes below those found in the F.V. model and in observations. However, there were no major differences in phase between the models, which were in general in good agreement with measurement. For the M_4 tide, the F.E. model had a slight bias to overestimate its amplitude, with significant differences between the observed and computed phase. In the case of the F.V. model, because the M_2 tide was underestimated compared to the F.E. model, the M_4 tide was also reduced, giving a slightly better agreement with observations. These differences in M_2 and M_4 amplitudes between the two models were reflected in the M_4 to M_2 ratio. However, both models had significant phase errors when compared to coastal gauges. In addition there were no systematic differences in either elevation or phase between the two models from one coastal location to another. A detailed examination of the two solutions in the eastern Irish Sea, away from the near shore region showed that they were comparable to each other. However in the near shore area, both solutions showed small scale variability in elevation and phase that was not consistent from one solution to another. This suggested that the mesh in this region was not sufficiently fine to accurately resolve the small scale spatial variability that occurs in the M_4 tide. In a separate study of tide-surge interaction, Xing et al. (2010) found significant spatial variability in the non-linear terms from one node to another in the near shore region. This clearly shows that the non-linear terms which are important for M_4 generation in the coastal region were not being accurately resolved on the present mesh in the coastal region, suggesting that a finer mesh was required in this area. In addition the "wetting and drying" algorithm can influence the tide in the near shore region particularly if the mesh is not sufficiently fine (Karna et al. 2011).

Comparison of the M_6 tide computed with both models showed significant differences over the eastern Irish Sea, with amplitudes computed with the F.V. model below those found with the F.E. model. Since the M_6 tide is primarily generated from the M_2 tide through the quadratic friction term

and to a certain extent from M_2 and M_4 interaction through the non-linear terms (see for example Jones and Davies (2010) and references therein for details), the fact that the M_2 tide computed with the F.V. model was below that computed with the F.E. model meant that the M_6 tide was appreciably less. In addition the short wavelength of the M_6 tide meant that there was significant spatial variability over the eastern Irish Sea, suggesting that a further refinement of the mesh could be useful. In addition as shown in the non-linear interaction study of Xing et al. (2010) in the near shore region there is significant spatial variability from one node to another in the quadratic friction term, suggesting that as for the M_4 tide a finer near shore mesh is required.

Calculations with a reduced value of k, namely k=0.0025, showed that the F.E. model significantly overestimates the M_2 tide, while the F.V. model consistently underestimates its value, although the phase of the tide was not appreciably influenced by this change in k. For the reasons discussed above, changes in the M_2 tide are reflected in the M_4 and M_6 tidal distributions. A further reduction of k to k=0.00125, in the F.V. model gave rise to an offshore displacement of the M_2 amphidromic point off the east coast of Ireland, with an associated increase of the order of 20cm in M_2 tidal amplitude in the eastern Irish Sea, but little change in phase. Although amplitudes were still slightly lower than those computed with the F.E. model, on average they agreed with observations with a comparable accuracy to those found with the F.E. model and k=0.003. The M_4 tide in the eastern Irish Sea was not substantially affected by this change in friction although the M_6 tidal distribution did change, since this constituent is primarily generated by bottom friction.

Calculations with a three dimensional (3D) version of the F.V. model with a minimum friction k=0.0025, and enhanced friction in shallow water, for the M_2 tide gave a comparable solution to the two dimensional (2D) version with k=0.00125. In addition this solution was in good agreement with observations in the eastern Irish Sea. In terms of the M_4 tide both calculations showed a similar distribution away from the coastal region, where the 3D version gave a slightly higher of order 2cm amplitude in the M_4 tide, and on average a slightly better agreement with observations. For the M_6 tide the 2D and 3D models gave different distributions over the eastern Irish Sea reflecting differences in bottom friction formulation, namely in terms of the depth mean current in the 2D model and bottom

current in the 3D model. The significant spatial variability in both the observed and computed M_6 tide suggested that on the present mesh the detailed model/data intercomparison presented in the Tables was rather inconclusive in terms of which model formulation was most accurate for the M_6 tide. Even if the mesh in the eastern Irish Sea was refined to improve its ability to resolve small spatial scale variations in the tide, it would be necessary to obtain an enhanced representation of bottom topography, which is not currently available. Also in the near shore region the form of the "wetting/drying" algorithm used in the model will influence the near coastal tidal distribution. In addition as shown by Aldridge and Davies (1993) bed types and bed forms vary significantly in the area, and in any detailed model skill assessment it would be necessary to use a spatially varying k reflecting this. As shown by Nicolle and Karpytchev (2007) such variations are important for tidal simulations in coastal regions although are currently not available over the whole domain presented here. However, despite this lack of a detailed knowledge of the spatial variability of k, and accurate near shore topography and an optimal "wetting/drying" condition, the calculations presented here show that for a given k there are differences in the tidal distributions computed with the F.E. and F.V. models, with the F.V. model having a larger dissipation than the F.E. model. In addition both models show similar changes to variations in k, with the 3D F.V. model giving an accurate representation of the tide with k=0.0025 over the deep water part of the model, and increasing in coastal regions.

Acknowledgements

The authors are indebted to Philip Hall for assitance with model runs on the cluster and Eleanor Ashton for typing text. We are grateful to the FVCOM developer for making the code available . The origin of the TELEMAC SYSTEM is EDF-LNHE and is therefore © EDF-LNHE.

Table 1: Summary of models and parameters used in the various calculations.

Calc.	Model	k	2D or 3D
1 (F.E.)	F.E.	0.003	2D
1 (F.V.)	F.V.	0.003	2D
2 (F.E.)	F.E.	0.0025	2D
2 (F.V.)	F.V.	0.0025	2D
3 (F.V.)	F.V.	0.00125	2D
4 (3D)	F.V.	Eqtn(1)	3D

Table 2: Comparison of observed amplitude (cms) and phase (degrees) (h_o, g_o) and computed (h_c, g_c), at the M_2 tidal frequency for various ports from calculations with F.E. and F.V. models (Calcs 1 to 4).

Point	Port	Observed		Calc 1 (F.E.)		Calc 1 (F.V.)		Calc 2 (F.E.)		Calc 2 (F.V.)		Calc 3(F.V.)		Calc 4(3D)	
		h0	g0	hc	gc	hc	gc	hc	gc	hc	gc	hc	gc	hc	gc
A	Barrow	308	331	311	329	214	329	327	327	219	327	232	324	279	326
B	Birkenhead	311	323	310	313	265	316	323	312	273	315	293	313	290	314
C	Douglas	230	326	235	314	202	320	246	313	209	320	226	320	223	322
D	Heysham	315	325	317	318	279	325	329	316	289	323	310	320	307	321
E	Hilbre	292	317	307	310	267	312	321	308	275	311	294	308	292	310
F	Liverpool	312	323	308	313	267	316	322	313	275	315	297	313	292	314
G	Formby	312	315	305	307	265	312	316	307	273	311	291	308	289	310
H	Hestan	275	339	274	322	242	332	287	321	251	332	273	330	268	331
I	Liverpool Bay	262	315	306	306	263	310	321	305	271	309	290	307	288	307
J	Ramsay	262	328	250	315	213	322	261	315	220	322	239	321	236	321
K	Workington	273	332	279	319	247	327	293	318	256	328	277	325	273	326
L	Wylfa Head	206	300	225	289	190	293	235	290	194	293	204	295	203	294
M	Liverpool (G.D.)	307	321	308	312	266	315	323	311	274	315	294	312	291	313
N	Llandudno	267	308	281	299	240	303	293	300	246	304	263	302	261	303
O	New Brighton	306	318	308	312	266	315	323	311	274	315	295	313	291	313
P	Amlwch	235	305	245	293	209	297	256	294	214	298	227	298	226	298
Q	OSTG	290	315	308	307	265	311	322	306	273	311	292	308	290	309
R	Queens Channel	296	316	307	307	264	311	322	306	272	311	291	308	289	309
S	STD Irish Sea	235	317	251	305	215	310	263	305	221	311	236	310	234	311
T	STN 10	262	318	277	306	238	312	290	306	245	312	262	311	260	311
U	STN 34	263	324	274	312	239	319	287	312	246	320	265	318	262	319
V	STN 35	255	332	266	319	233	328	279	318	241	328	260	326	256	327
W	Creetown	233	342	255	327	228	336	265	326	236	335	253	333	248	334
X	Conwy	241	318	217	299	186	304	224	299	190	303	200	303	196	303
Y	Barrow RI	306	329	156	322	134	326	163	321	138	325	149	323	147	324
Z	Barrow HP	292	327	308	324	272	327	324	321	281	325	305	322	300	324
AA	Barrow HS	297	325	301	314	266	320	317	315	274	319	296	317	292	319
BB	Morecambe	308	326	283	329	231	337	298	325	242	334	276	329	260	333
CC	Fleetwood	305	326	191	322	180	323	202	323	186	322	200	319	196	320

Table 3: Comparison of observed amplitude (cm) and phase (degrees; h_o, g_o) and computed (h_c, g_c) at the M_4 tidal frequency for various ports from calculations with F.E. and F.V. models (Calcs 1 to 4).

Point	Port	Observed		Calc 1 (F.E.)		Calc 1 (F.V.)		Calc 2 (F.E.)		Calc 2 (F.V.)		Calc 3 (F.V.)		Calc 4 (3D)	
		h0	g0	hc	gc	hc	gc	hc	gc	hc	gc	hc	gc	hc	gc
A	Barrow	19	252	38	207	36	281	38	203	37	282	42	282	41	280
B	Birkenhead	23	217	28	154	19	149	27	150	19	142	19	110	22	133
C	Douglas	6	233	7	177	6	195	7	170	6	191	6	171	7	184
D	Heysham	20	243	11	194	12	159	9	216	11	153	4	135	11	154
E	Hilbre	20	203	27	165	19	159	28	160	19	153	18	125	22	140
F	Liverpool	23	214	30	154	21	151	30	150	22	146	21	118	25	138
G	Formby	25	235	19	156	16	154	18	158	17	148	16	124	19	137
H	Hestan	12	280	12	176	12	196	12	167	13	189	13	166	14	180
I	Liverpool Bay	21	196	20	151	15	153	20	142	16	146	16	117	18	132
J	Ramsay	7	237	10	163	9	179	10	154	10	173	10	151	11	165
K	Workington	13	253	13	173	13	189	13	166	14	183	14	159	16	173
L	Wylfa Head	4	182	2	160	1	62	2	195	1	20	3	324	3	340
M	Liverpool (G.D.)	22	202	33	157	23	156	33	152	24	150	24	128	27	143
N	Llandudno	12	181	13	138	10	141	13	130	10	134	10	106	11	120
O	New Brighton	23	198	32	158	23	156	32	154	23	151	24	128	27	144
P	Amlwch	6	185	6	144	4	139	6	143	4	133	2	100	3	113
Q	OSTG	17	196	21	152	16	153	22	144	17	147	17	117	19	133
R	Queens Channel	17	197	21	154	16	153	22	147	16	147	17	118	19	133
S	STD Irish Sea	6	201	8	149	6	156	8	142	7	151	7	126	7	140
T	STN 10	16	199	13	150	10	156	13	143	11	149	11	123	12	137
U	STN 34	11	217	13	156	12	168	13	149	13	162	14	137	15	151
V	STN 35	11	248	11	168	12	186	11	160	12	179	13	156	14	171
W	Creetown	30	274	30	208	25	215	27	206	26	211	21	194	27	212
X	Conwy	26	216	39	223	35	223	40	223	35	223	33	225	37	224
Y	Barrow RI	30	274	66	284	56	290	70	281	57	288	62	286	61	286
Z	Barrow HP	26	216	31	203	8	171	28	195	8	164	5	107	10	155
AA	Barrow HS	16	200	14	180	11	174	16	176	11	168	10	142	13	157
BB	Morecambe	11	217	33	244	29	255	33	246	30	254	33	250	34	249
CC	Fleetwood	11	248	63	261	52	267	68	254	53	266	56	265	56	264

Table 4: Comparison of observed amplitude (cm) and phase (degrees; ho, go) and computed (hc, gc) at the M_6 tidal frequency for various ports from calculations with F.E. and F.V. models (Calcs 1 to 4).

Point	Port	Observed		Calc 1 (F.E.)		Calc 1 (F.V.)		Calc 2 (F.E.)		Calc 2 (F.V.)		Calc 3 (F.V.)		Calc 4 (3D)	
		h0	g0	hc	gc	hc	gc	hc	gc	hc	gc	hc	gc	hc	gc
A	Barrow	3	49	13	41	21	108	14	35	22	102	23	83	24	97
B	Birkenhead	5	321	15	323	10	338	16	323	11	334	14	319	12	327
C	Douglas	1	354	1	72	0	316	1	67	1	29	1	82	1	103
D	Heysham	2	11	8	300	6	304	5	315	6	303	5	291	5	299
E	Hilbre	2	33	7	331	5	338	7	332	5	340	2	355	2	355
F	Liverpool	5	322	14	327	9	343	15	325	9	341	11	327	10	336
G	Formby	5	11	6	331	4	341	7	359	4	342	3	10	3	18
H	Hestan	-	-	1	113	2	203	1	72	2	180	4	87	2	112
I	Liverpool Bay	-	-	6	311	4	338	6	311	4	341	2	349	2	2
J	Ramsay	-	-	2	110	1	196	1	101	1	184	2	107	1	139
K	Workington	2	325	1	173	2	221	1	126	2	207	3	81	1	107
L	Wylfa Head	-	-	1	205	0	324	0	178	1	357	1	3	1	40
M	Liverpool (G.D.)	5	349	13	326	8	341	14	324	8	339	9	322	8	334
N	Llandudno	2	356	3	289	3	321	3	289	2	327	2	350	1	13
O	New Brighton	5	329	13	325	8	341	14	324	8	339	8	323	8	334
P	Amlwch	-	-	1	248	1	330	1	271	1	347	1	3	1	33
Q	OSTG	4	14	6	315	5	342	6	318	4	345	2	345	2	2
R	Queens Channel	3	18	6	318	5	342	7	321	4	343	2	349	2	2
S	STD Irish Sea	1	354	2	287	1	316	1	296	1	323	1	352	1	9
T	STN 10	3	335	3	300	3	326	3	306	2	330	1	349	1	358
U	STN 34	1	7	2	310	1	309	2	315	1	318	2	45	1	35
V	STN 35	1	234	1	119	2	184	1	93	2	167	4	91	2	113
W	Creetown	5	117	12	66	6	93	13	65	7	88	12	83	11	87
X	Conwy	6	22	21	11	19	11	22	8	19	11	20	8	21	13
Y	Barrow RI	5	117	4	170	3	138	6	164	3	124	2	27	3	116
Z	Barrow HP	6	22	10	16	1	314	14	0	2	324	4	316	3	315
AA	Barrow HS	3	355	6	320	5	335	6	315	5	333	5	307	4	318
BB	Morecambe	1	7	17	24	14	44	16	15	15	38	16	6	15	29
CC	Fleetwood	1	234	8	103	12	77	8	108	13	72	13	63	14	72

Table 5: Ratio of M_4 to M_2 tidal amplitude ($x10^2$) for various ports from calculations with F.E. and F.V. models.

Point	Port	Calc 1 (F.E.)	Calc 1 (F.V.)	Calc 2 (F.E.)	Calc 2 (F.V.)
A	Barrow	12.2	16.8	11.6	16.9
B	Birkenhead	9.0	7.2	8.4	6.9
C	Douglas	2.9	2.9	2.8	2.9
D	Heysham	3.4	4.3	2.7	3.8
E	Hilbre	8.8	7.1	8.7	6.9
F	Liverpool	9.7	7.8	9.3	8.0
G	Formby	6.2	6.0	5.7	6.2
H	Hestan	4.4	4.9	4.2	5.2
I	Liverpool Bay	6.5	5.7	6.2	5.9
J	Ramsay	4.0	4.2	3.8	4.5
K	Workington	4.6	5.3	4.4	5.5
L	Wylfa Head	-	-	-	-
M	Liverpool (G.D.)	10.7	8.6	10.2	8.8
N	Llandudno	4.6	4.2	4.4	4.1
O	New Brighton	10.4	8.6	9.9	8.4
P	Amlwch	2.4	-	2.3	-
Q	OSTG	6.8	6.0	6.8	6.2
R	Queens Channel	6.8	6.0	6.8	5.9
S	STD Irish Sea	3.2	2.8	3.0	3.2
T	STN 10	4.7	4.2	4.5	4.5
U	STN 34	4.7	5.0	4.5	5.3
V	STN 35	4.1	5.1	3.9	5.0
W	Creetown	11.8	11.0	10.2	11.0
X	Conwy	18.0	18.8	17.9	18.4
Y	Barrow RI	42.3	41.8	42.9	41.3
Z	Barrow HP	10.1	2.9	8.6	2.8
AA	Barrow HS	4.7	4.1	5.0	4.0
BB	Morecambe	11.7	12.6	11.1	12.4
CC	Fleetwood	33.0	28.9	33.7	28.5

Table 6: Ratio of M_6 to M_2 tidal amplitudes ($x10^2$) for various ports from calculations with F.E. and F.V. models.

Point	Port	Calc 1 (F.E.)	Calc 1 (F.V.)	Calc 2 (F.E.)	Calc 2 (F.V.)
A	Barrow	4.2	9.8	4.3	10.0
B	Birkenhead	4.8	3.8	5.0	4.0
C	Douglas	-	-	-	-
D	Heysham	2.5	2.2	-	2.1
E	Hilbre	2.3	-	2.2	-
F	Liverpool	4.5	3.4	4.7	3.3
G	Formby	2.0	-	2.2	-
H	Hestan	-	-	-	-
I	Liverpool Bay	2.0	-	1.9	-
J	Ramsay	-	-	-	-
K	Workington	-	-	-	-
L	Wylfa Head	-	-	-	-
M	Liverpool (G.D.)	4.2	3.0	4.3	2.9
N	Llandudno	-	-	-	-
O	New Brighton	4.2	3.0	4.3	2.9
P	Amlwch	-	-	-	-
Q	OSTG	1.9	-	1.9	-
R	Queens Channel	1.9	-	2.2	-
S	STD Irish Sea	-	-	-	-
T	STN 10	-	-	-	-
U	STN 34	-	-	-	-
V	STN 35	-	-	-	-
W	Creetown	4.7	2.6	4.9	3.0
X	Conwy	9.7	10.2	9.8	10.0
Y	Barrow RI	-	-	3.7	-
Z	Barrow HP	3.2	-	4.3	-
AA	Barrow HS	2.0	-	1.9	-
BB	Morecambe	6.0	4.9	5.4	6.2
CC	Fleetwood	4.2	6.7	4.0	7.0

Figure Captions

Fig. 1: (a) Topography for the whole model domain and location of specific regions, (b) expanded plot of the eastern Irish Sea topography and place name locations, (c) positions of eastern Irish Sea gauges used in comparison tables.

Fig.2: Unstructured mesh used in the finite element (F.E.) and finite volume (F.V.) calculations.

Fig. 3: Computed co-tidal chart determined with the F.E. code (Calc 1 (F.E.) , k=0.003) (a) M_2 tide, (b) M_4 tide, and (c) M_6 tide over the whole region (i) and eastern Irish Sea (ii).

Fig. 4: Computed difference between tidal solutions derived using the F.E. and F.V. codes (namely Calc 1(F.E.)-Calc 1(F.V.), k=0.003) for (a) M_2 tide, (b) M_4 tide, and (c) M_6 tide over the whole region (i) and eastern Irish Sea (ii).

Fig. 5: Computed co-tidal charts determined with the F.V. code (Calc 2(F.V.), k=0.0025) (a)M_2 tide over the whole region (i) and eastern Irish Sea (ii), (b) M_4 tide and (c) M_6 tide over the eastern Irish Sea.

Fig. 6: Computed co-tidal chart determined with the F.V. code (Calc 3 (F.V.), k=0.00125) (a) M_2 tide, over the whole region (i) and eastern Irish Sea (ii), (b) M_4 tide and (c) M_6 tide over the eastern Irish Sea.

Fig. 7: Computed co-tidal chart determined with the three dimensional F.V. code (Calc 4(3D)) (a)M_2 tide over the whole region (i) and eastern Irish Sea (ii), (b) M_4 tide and (c) M_6 tide over the eastern Irish Sea.

References

Aldridge, J.N. and Davies, A.M. (1993) A high resolution three-dimensional hydrographic tidal model of the eastern Irish Sea. Journal of Physical Oceanography, 23, 207-224.

Chen, C., Huang, H., Beardsley, R.C., Liu, H., Xu, Q., Cowles, G. (2007) A finite volume numerical approach for coastal ocean circulation studies: Comparisons with finite difference models, J. Geophys. Res., 112, C03018, doi:10.1029/2006JC003485.

Chen, C., Liu, H., Beardsley, R.C. (2003) An unstructured grid, finite-volume, three-dimensional, primitive equations ocean model: Application to coastal ocean and estuaries. Journal of Atmospheric and Oceanic Technology 20, 159-186.

Chen, C., Qi, J., Li, C., Beardsley, R.C., Lin, H., Walker, R., and Gates, K. (2008) Complexity of the flooding/drying process in an estuarine tidal-creek salt-marsh system: an application of FVCOM. Journal of Geophysical Research 113, C07052 doi:10.1029/2007 JC004328.

Davies, A.M. (1986) A three-dimensional model of the northwest European continental shelf with application to the M_4 tide. Journal of Physical Oceanography, 16, 797-813.

Davies, A.M. and Aldridge, J.N. (1993) A numerical model study of parameters influencing tidal currents in the Irish Sea. Journal of Geophysical Research (Oceans) 98, 7049-7067.

Davies, A.M. and Jones, J.E. (1992) A three dimensional model of the M_2, S_2, N_2, K_1 and O_1 tides in the Celtic and Irish Sea. Progress in Oceanography, 29, 197-234.

Davies, A.M., Hall, P., Howarth, M.J., Knight, P and Player, R. (2001) Comparison of observed (HF Radar and ADCP measurements) and computed tides in the North Channel of the Irish Sea, Journal of Physical Oceanography, 31, 1764-1785.

Davies, A.M. and Kwong, S.C.M. (2000) Tidal energy fluxes and dissipation on the European continental shelf. Journal of Geophysical Research (Oceans), 105, 21, 967-21,989.

Davies, A.M. and Lawrence, J (1995) Modeling the effect of wave-current interaction on the three-dimensional wind-driven circulation of the eastern Irish Sea. Journal of Physical Oceanography, 25, 29-45.

Filloux, J.H., and Snyder, R.L. (1979) A study of tides, setup and bottom friction in a shallow semi-enclosed basin. Part I: Field experiment and harmonic analysis. Journal of Physical Oceanography, 9, 158-169.

Foreman, M.G.G., Henry, R.F., Walters, R.A., and Ballantyne, V.A. (1993) A finite element model for tides and resonance along the north coast of British Columbia. Journal of Geophysical Research, 98, 2509-2531.

Foreman, M.G.G., Walters, R.A., Henry, R.F., Keller, C.P., and Dolling, A.G. (1995) A tidal model for eastern Juan de Fuca Strait and the southern Strait of Georgia. Journal of Geophysical Research, 100, 721-740.

Fortunato, A.B., Baptista, A.M. and Luettich, R.A. (1997) A three-dimensional model of tidal currents in the mouth of the Tagus estuary. Continental Shelf Research, 17, 1689-1714.

George, K.J. (1980) Anatomy of an amphidrome. Hydrographic Journal, 18, 5-12.

Greenberg, D.A., Dupont, F., Lyard, F.H., Lynch, D.R. and Werner, F.E. (2007) Resolution issues in numerical models of oceanic and coastal circulation. Continental Shelf Research, 27, 1317-1343.

Greenberg, D.A., Shore, J.A., Page, F.H., and Dowd, M. (2005) Finite element circulation model for embayments with drying intertidal areas and its application to the Quoddy region of the Bay of Fundy. Ocean Modelling, 10, 211-231.

Heaps, N.S. (1978) Linearized vertically-integrated equations for residual circulation in coastal seas. Dtsch. Hydrogr. Z. 31, 147-169.

Hervouet, J-M (2002) TELEMAC modelling system: an overview. Hydrological Processes, 14, 2209-2210.

Huang, H., Chen, C., Blanton, J.O., and Andrade, F.A. (2008) A numerical study of tidal asymmetry in Okatee Creek, South Carolina. Estuarine Coastal and Shelf Science, 78, 190-202.

Inoue, R., and Garrett, C. (2007) Fourier Representation of Quadratic friction. Journal of Physical Oceanography, 37, 593-610.

Ip, J.T.C., Lynch, D.R. and Friedrichs, C.T. (1998) Simulation of Estuarine flooding and dewatering with application to Great Bay, New Hampshire. Estuarine Coastal and Shelf Science, 47, 119-141.

Jones, J.E. (1983) Charts of the O_1, K_1, N_2, M_2 and S_2 tides in the Celtic Sea including M_2 and S_2 tidal currents. Institute of Oceanographic Sciences, Report No. 169, 55pp.

Jones, J E and Davies, A M (1996) A high resolution three dimensional model of the M_2, M_4, M_6, S_2, N_2, K_1, and O_1 tides in the eastern Irish Sea. Estuarine Coastal and Shelf Science 42, 311-346.

Jones, J.E. (2002) Coastal and shelf-sea modelling in the European context. Oceanography and Marine Biology: an Annual Review, 40, 37-141.

Jones, J.E. and Davies, A.M. (2005) An intercomparison between finite difference and finite element (TELEMAC) approaches to modelling west coast of Britain tides. Ocean Dynamics, 55, 178-199.

Jones, J.E. and Davies, A.M. (2007) On the sensitivity of tidal residuals off the west coast of Britain to mesh resolution. Continental Shelf Research, 27, 64-81.

Jones, J.E. and Davies, A.M (2010) Application of a finite element model to the computation of tides in the Mersey estuary and Eastern Irish Sea. Continental Shelf Research 30, 491-514.

Jones, J.E., Hall, P. and Davies, A.M (2009) An intercomparison of tidal solutions computed with a range of unstructured grid models of the Irish and Celtic Sea regions. Ocean Dynamics, 59, 997-1023.

Karna, T., de Brye, B., Gourgue, O., Lambrechts, J., Comblen, R., Legat, V., and Deleersnijder, E (2011) A fully implicit wetting-drying method for DG-FEM shallow water models, with an application to the Scheldt Estuary. Computer Methods in Applied Mechanics and Engineering 200, 509-524.

Kwong, S.C.M., Davies, A.M. and Flather, R.A. (1997) A three dimensional model of the principal tides on the European Shelf. Progress in Oceanography, 39, 205-262.

Legrand, S. Deleersnijder, E., Hanert, E., Legat, V. and Wolanski, E. (2006) High-resolution, unstructured meshes for hydrodynamic models of the Great Barrier Reef, Australia. Estuarine, Coastal and Shelf Science, 68, 36-46.

Legrand, S. Deleersnijder, E., Delhez, E. and Legat, V. (2007) Unstructured, anisotropic mesh generation for the Northwestern European continental shelf, the continental slope and the neighbouring ocean. Continental Shelf Research, 27, 1344-1356.

LeProvost, C. (1991) Generation of overtides and compound tides (review). Tidal Hydrodynamics, B.B. Parker (Editor). Published John Wiley and Sons 269-295.

LeProvost, C. and Fornerino, M. (1985) Tidal spectroscopy of the English Channel with a numerical model. Journal of Physical Oceanography, 15, 1009-1031.

Levasseur, A., Shi, L., Wells, N.C., Purdie, D.A. and Kelly-Gerreyn, B.A. (2007) A three-dimensional hydrodynamic model of estuarine circulation with an application to Southampton water, U.K. Estuarine Coastal and Shelf Science, 73, 753-767.

Lynch, D.R. and Naimie, C.E. (1993) The M_2 tide and its residual on the outer banks of the Gulf of Maine. Journal of Physical Oceanography, 23, 2222-2253.

Lynch, D.R., Smith, K.W., and Cahill, B. (2004) Seasonal Mean Circulation on the Irish Shelf – A Model-Generated Climatology, Continental Shelf Research 24:18, 2215-2244.

Malcherek, A. (2000) Application of TELEMAC-2D in a narrow estuarine tributary. Hydrological Processes, 14, 2293-2300.

Nicolle, A. and Karpytchev, M. (2007) Evidence for spatially variable friction from tidal amplification and asymmetry in a shallow semi-diurnal embayment: the Pertuis Breton Bay of Biscay, France. Continental Shelf Research, 27, 2346-2356.

Robinson, I.S. (1979) The tidal dynamics of the Irish and Celtic Seas. Geophysical Journal of the Royal Astronomical Society, 56, 159-197.

Walters, R.A. and Werner, F.E. (1991) Nonlinear generation of overtides, compound tides, and residuals. Pg 297-320 in Tidal Hydrodynamics edited B.B. Parker, published John Wiley and Sons.

Walters, R.A. (1992) A three-dimensional, finite element model for coastal and estuarine circulation. Continental Shelf Res., 12, 83-102.

Walters, R.A. (2005) Coastal ocean models: two useful finite element methods. Continental Shelf Research, 25, 775-793.

Werner, F.E. (1995) A field test case for tidally forced flows: a review of the tidal flow forum pg. 269-284 in Quantitative Skill Assessment for Coastal Ocean Models, ed. D.R. Lynch and A.M. Davies, published American Geophysical Union.

Xing, J., Jones, J.E., Davies, A.M. and P. Hall (2010) Modelling tide-surge interaction effects using finite volume and finite element models of the Irish Sea (submitted).

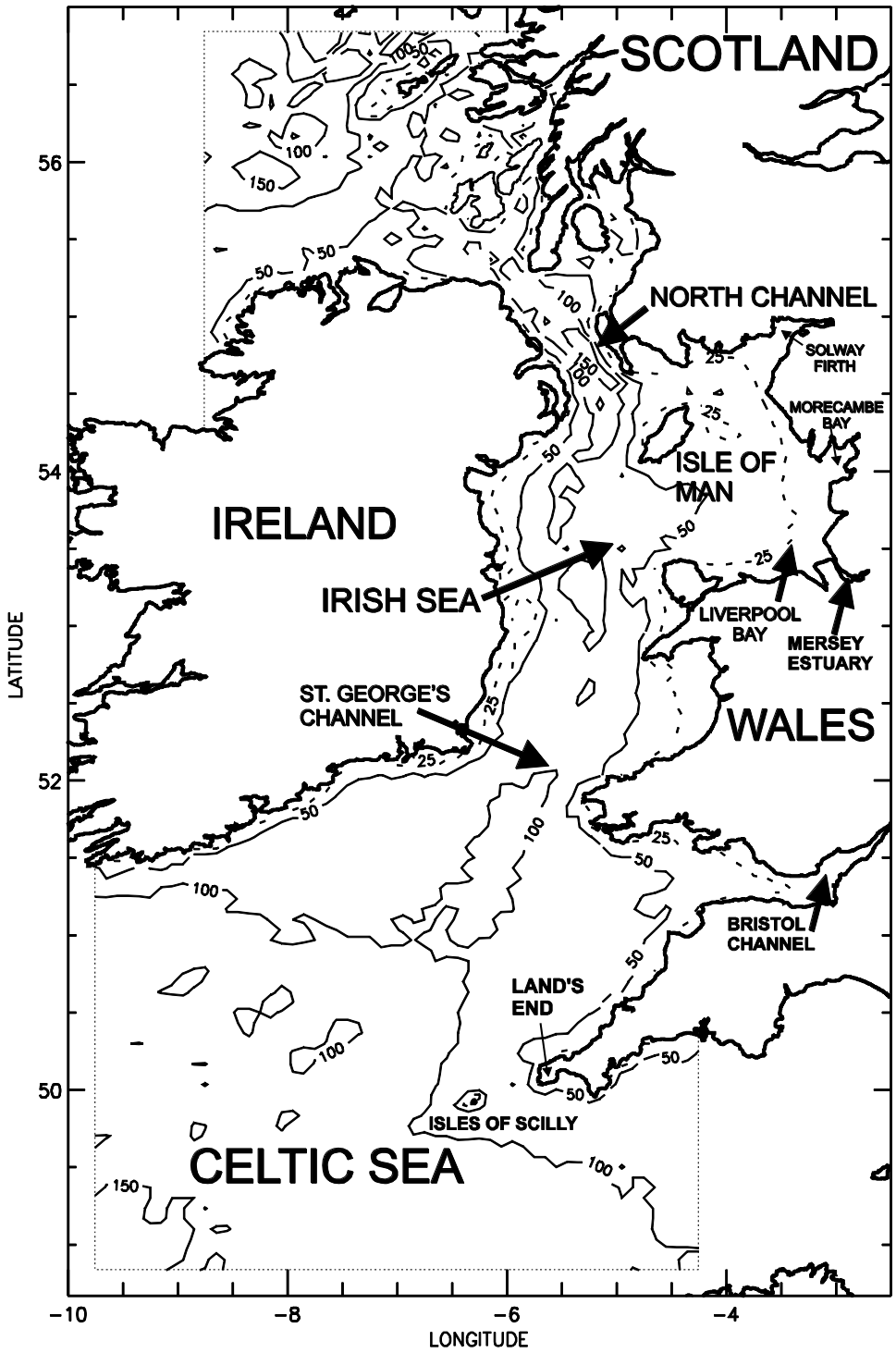
SCOTLAND
NORTH CHANNEL
SOLWAY FIRTH
MORECAMBE BAY
ISLE OF MAN
IRELAND
IRISH SEA
LIVERPOOL BAY
MERSEY ESTUARY
ST. GEORGE'S CHANNEL
WALES
BRISTOL CHANNEL
LAND'S END
ISLES OF SCILLY
CELTIC SEA
LATITUDE
LONGITUDE
56
54
52
50
−10
−8
−6
−4
25
50
100
150

Fig.1a

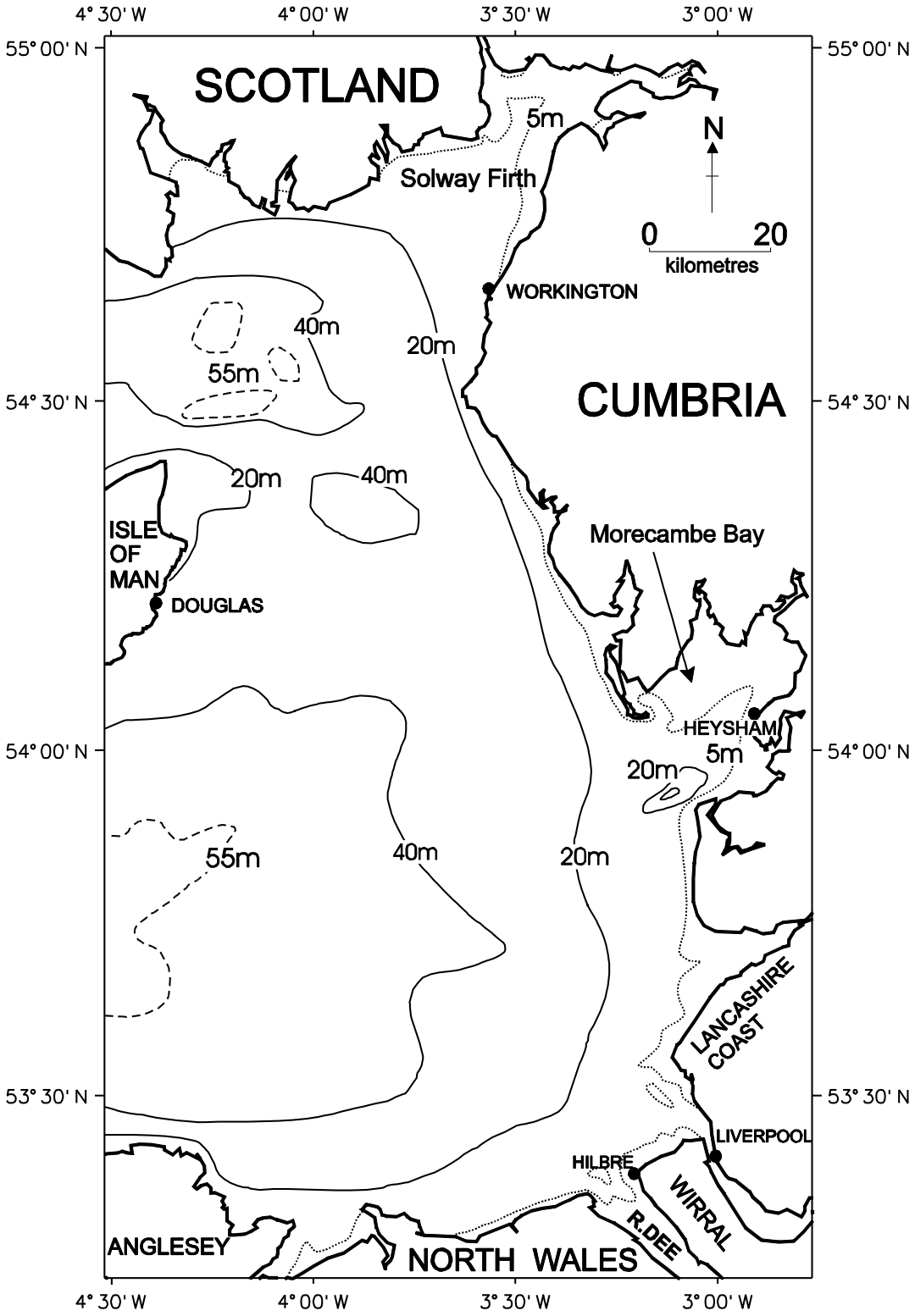
4° 30' W
4° 00' W
3° 30' W
3° 00' W
55° 00' N
54° 30' N
54° 00' N
53° 30' N
SCOTLAND
5m
Solway Firth
N
0
20
kilometres
WORKINGTON
40m
20m
55m
CUMBRIA
20m
40m
ISLE
OF
MAN
DOUGLAS
Morecambe Bay
HEYSHAM
5m
20m
55m
40m
20m
LANCASHIRE
COAST
LIVERPOOL
HILBRE
WIRRAL
R.DEE
ANGLESEY
NORTH WALES

Fig. 1b

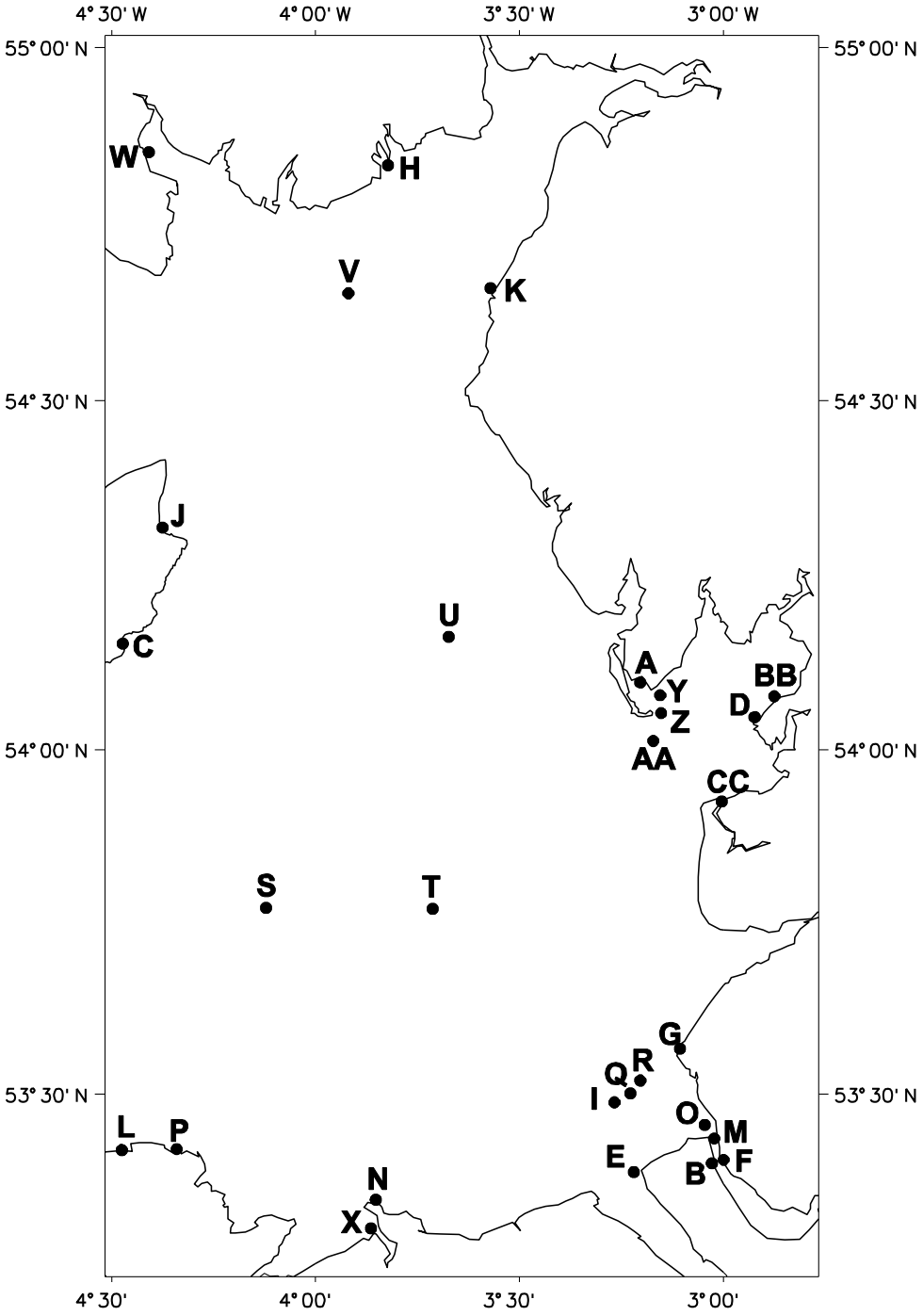
4° 30' W
4° 00' W
3° 30' W
3° 00' W
55° 00' N
54° 30' N
54° 00' N
53° 30' N
4° 30'
4° 00'
3° 30'
3° 00'
W
H
V
K
J
C
U
A
Y
Z
AA
BB
D
CC
S
T
G
Q
R
I
O
M
E
F
B
L
P
N
X

Fig.1c

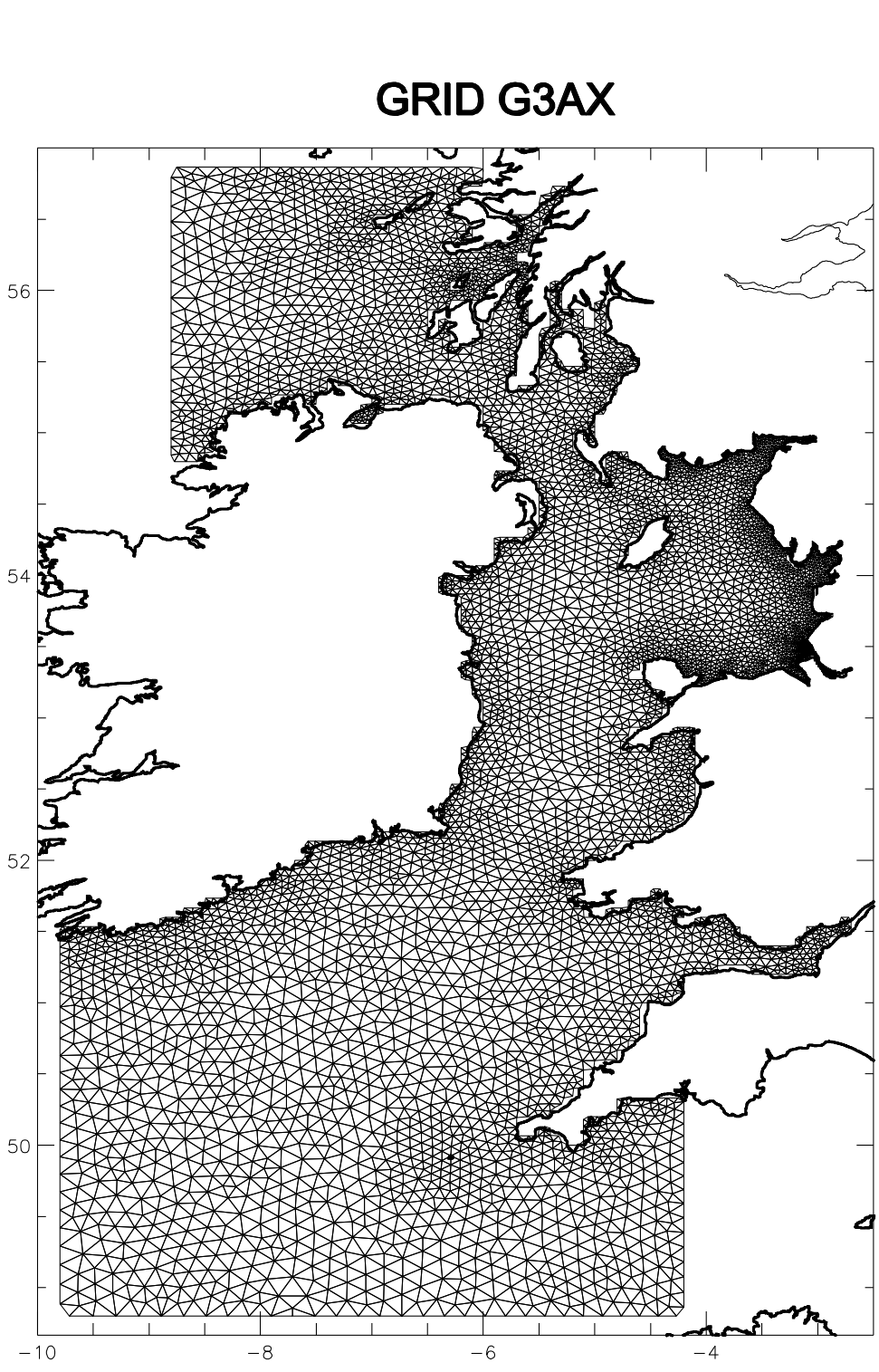

Fig.2

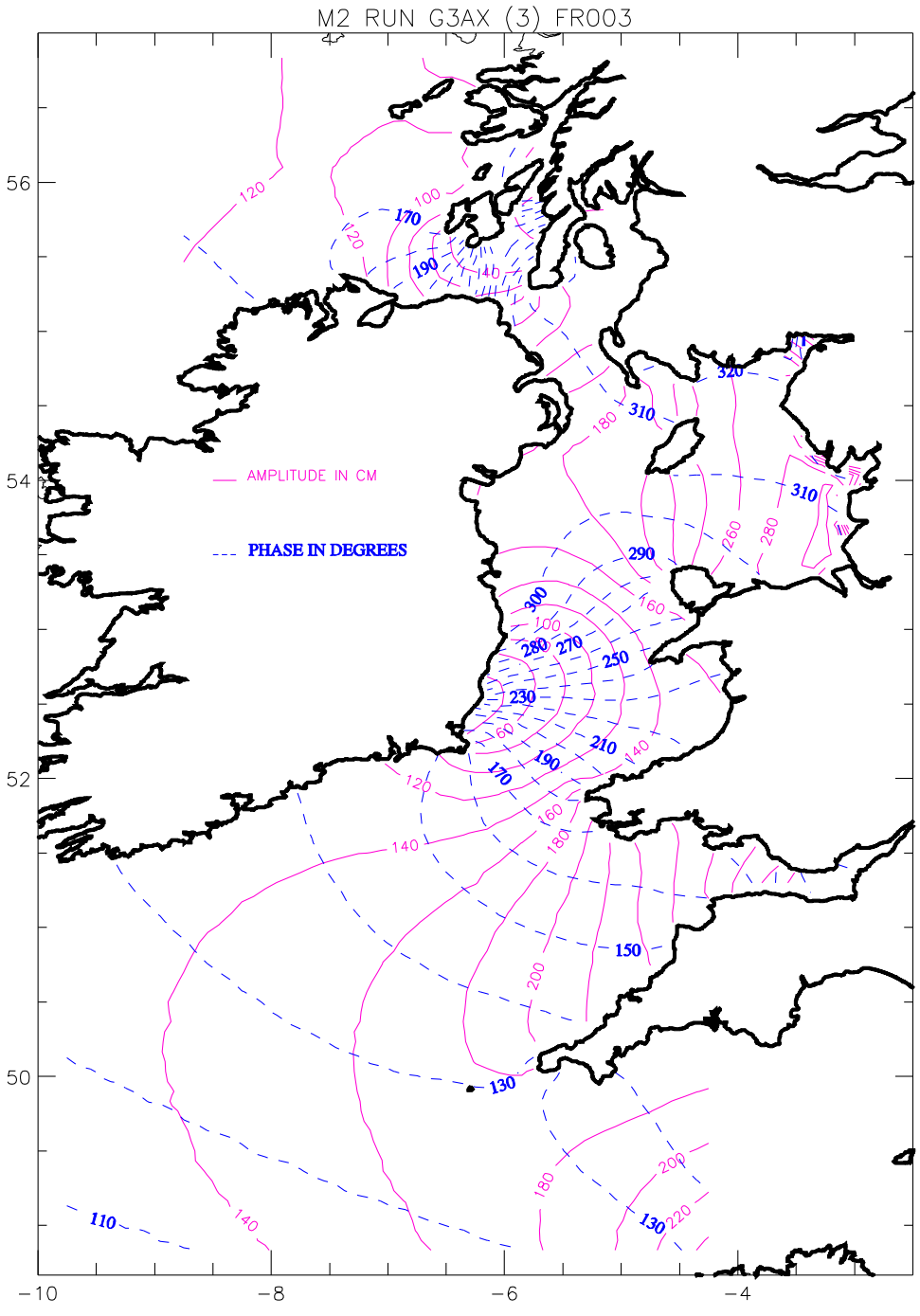
M2 RUN G3AX (3) FR003
AMPLITUDE IN CM
PHASE IN DEGREES
56
54
52
50
−10
−8
−6
−4

Fig. 3a(i)

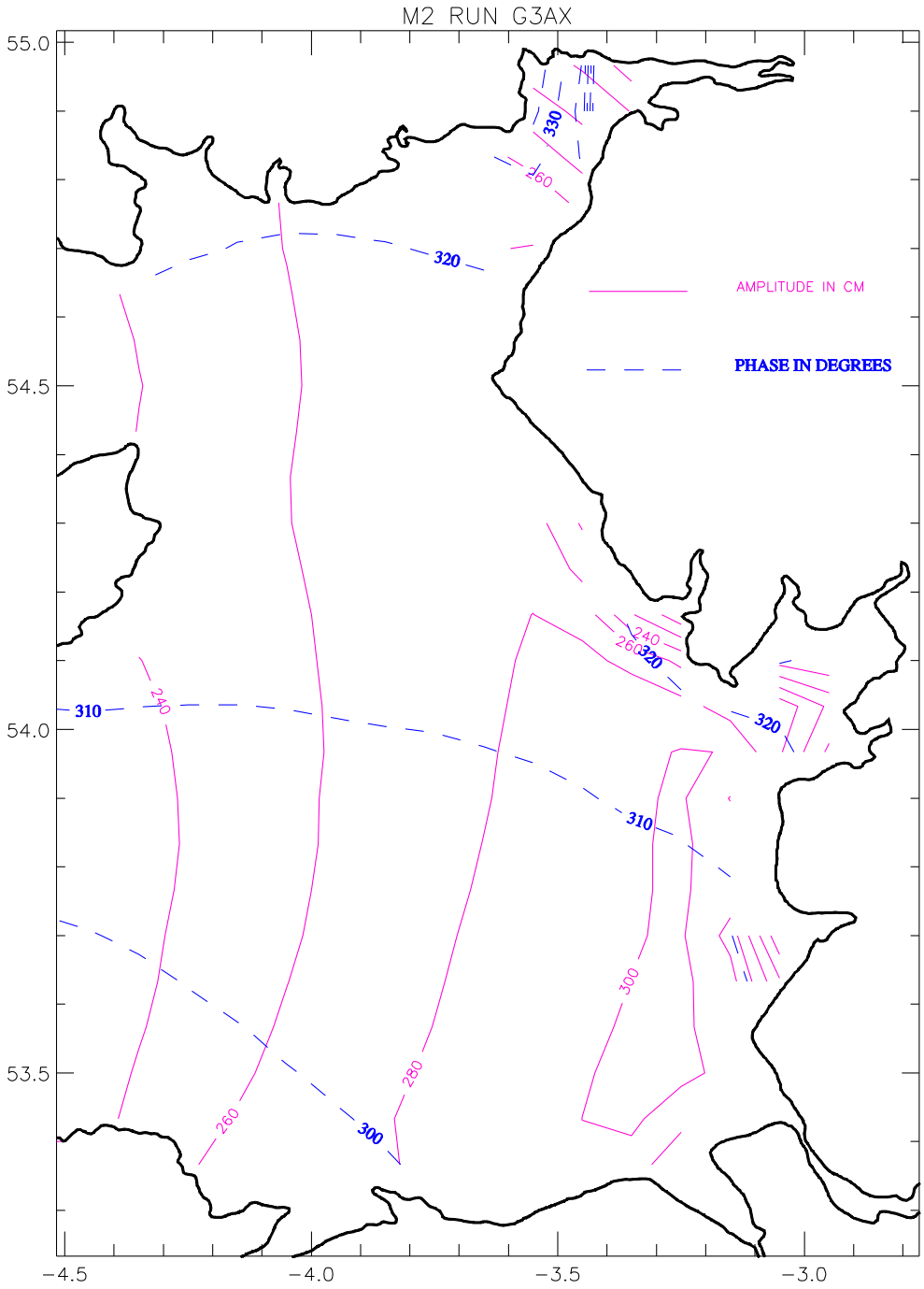
M2 RUN G3AX
55.0
54.5
54.0
53.5
−4.5
−4.0
−3.5
−3.0
AMPLITUDE IN CM
PHASE IN DEGREES
330
320
310
300
260
240
280

Fig. 3a(ii)

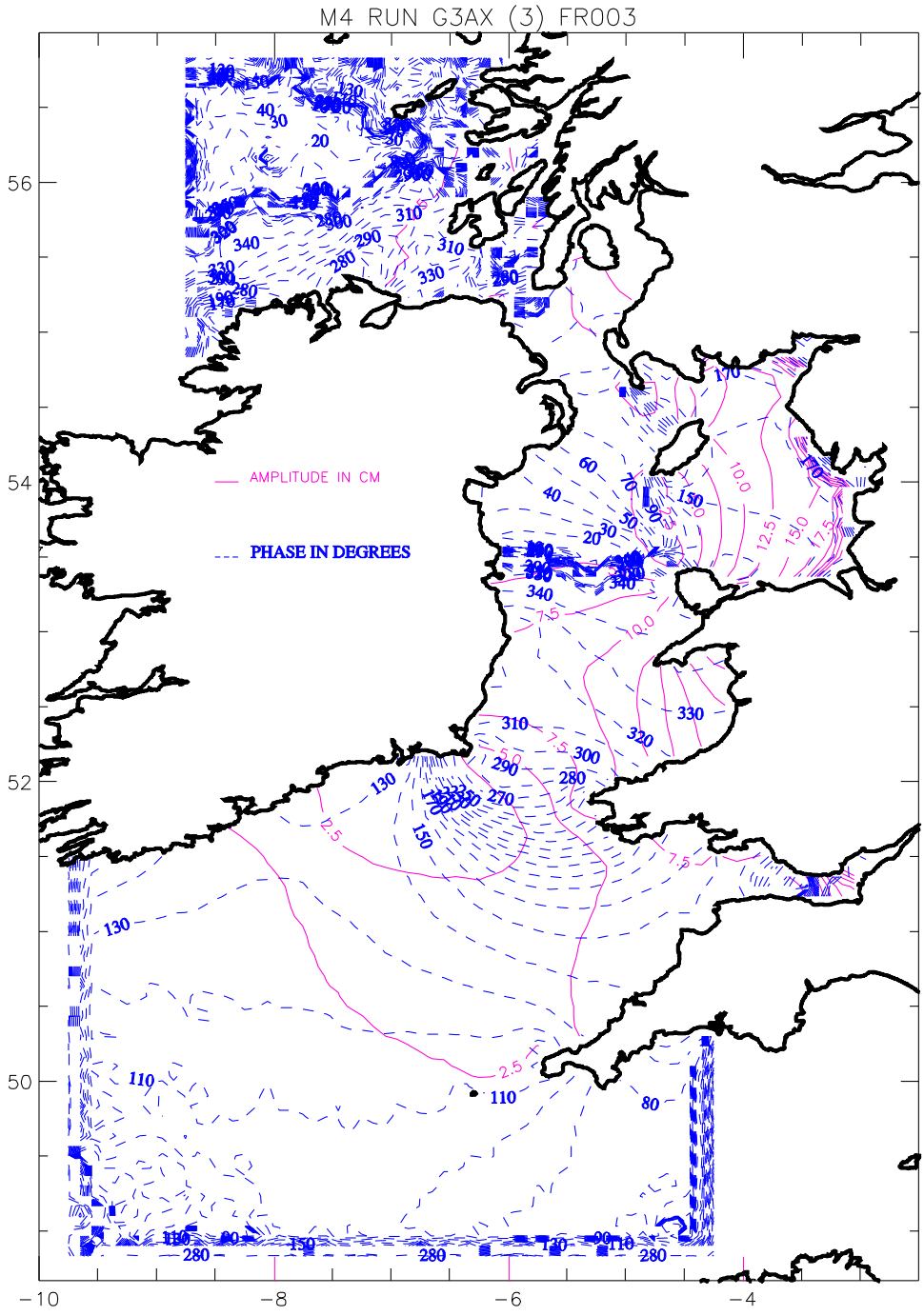
M4 RUN G3AX (3) FR003
AMPLITUDE IN CM
PHASE IN DEGREES
56
54
52
50
−10
−8
−6
−4

Fig. 3b(i)

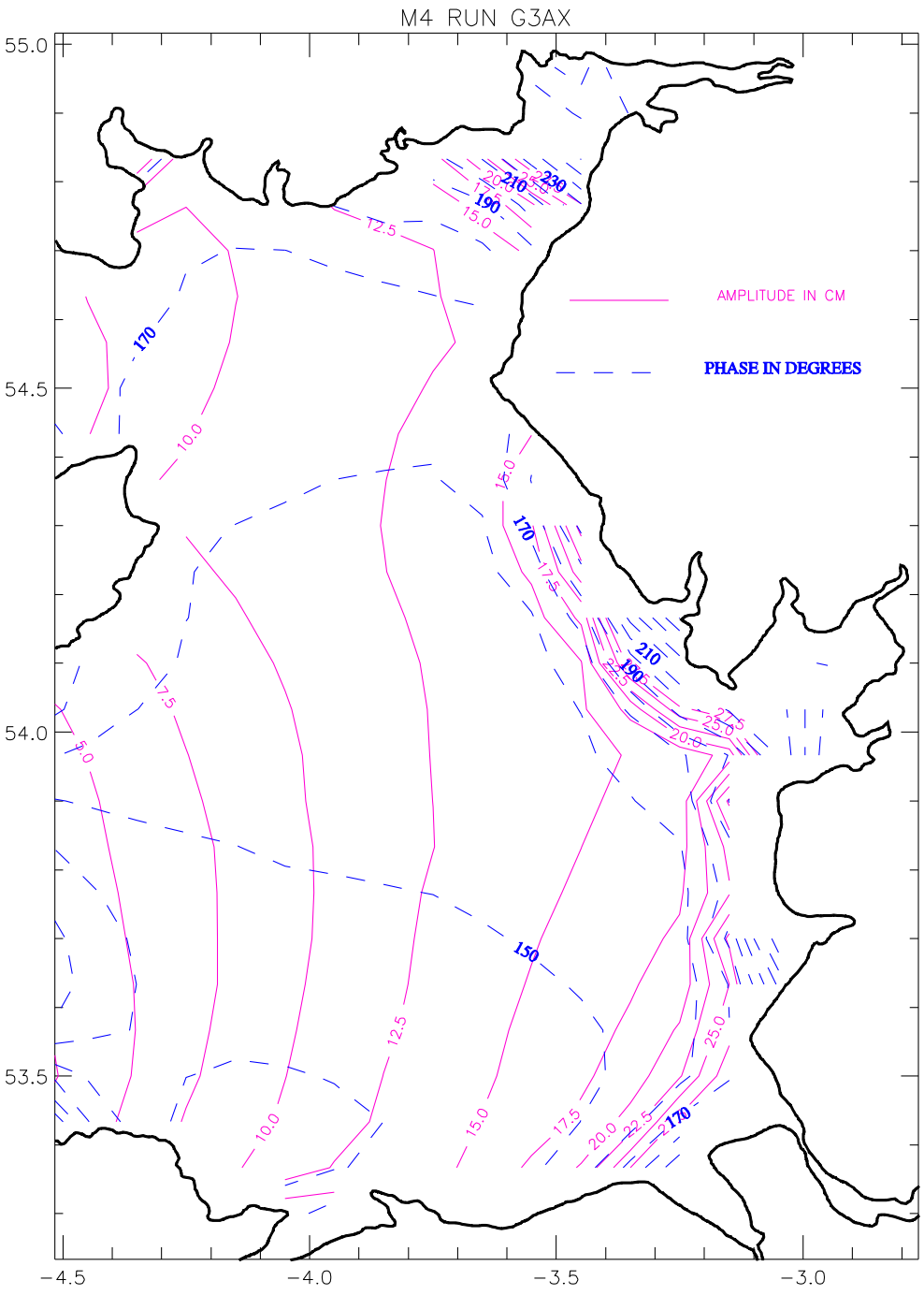
M4 RUN G3AX
AMPLITUDE IN CM
PHASE IN DEGREES
55.0
54.5
54.0
53.5
−4.5
−4.0
−3.5
−3.0

Fig.3b(ii)

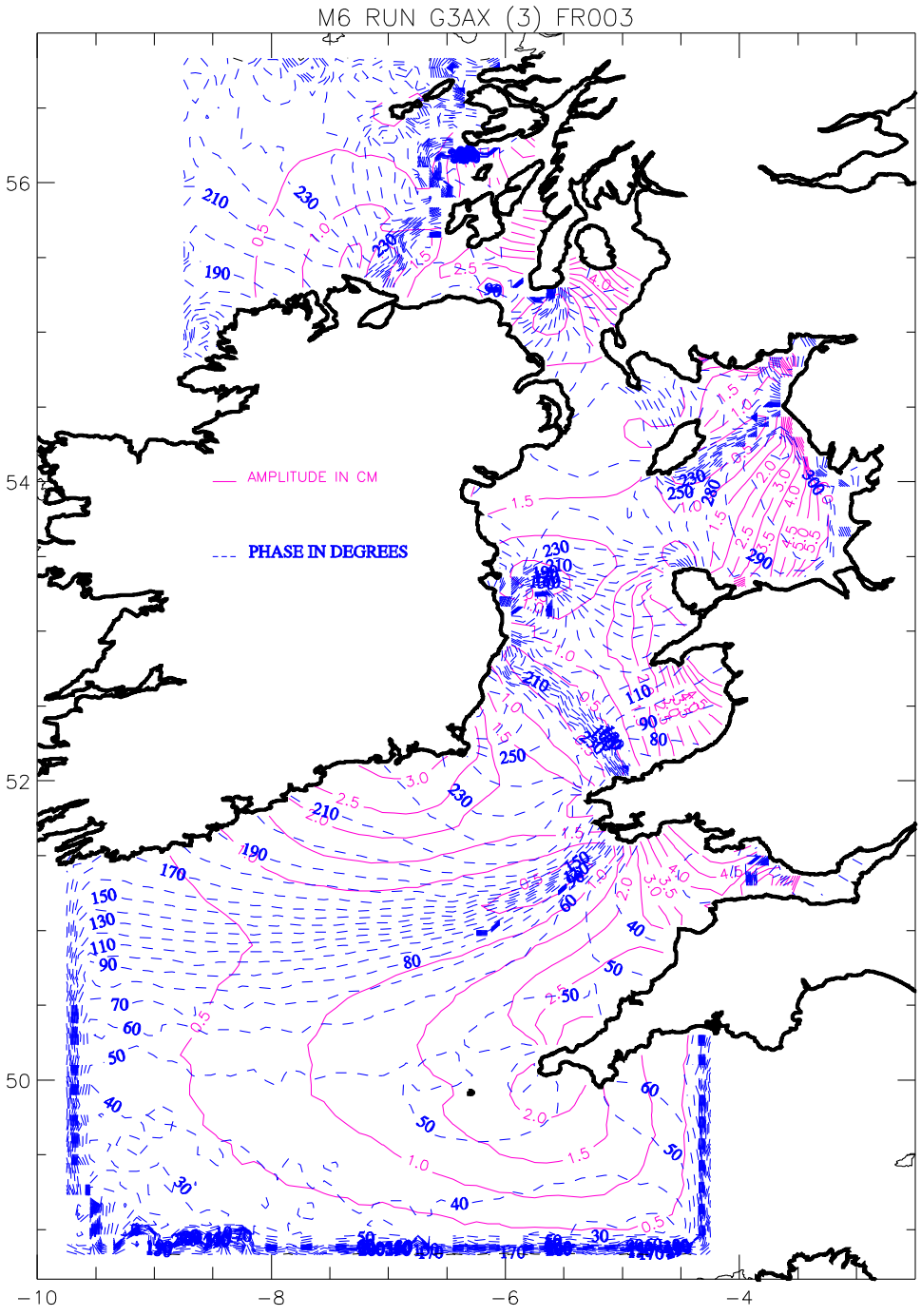
M6 RUN G3AX (3) FR003
AMPLITUDE IN CM
PHASE IN DEGREES
56
54
52
50
−10
−8
−6
−4

Fig.3c(i)

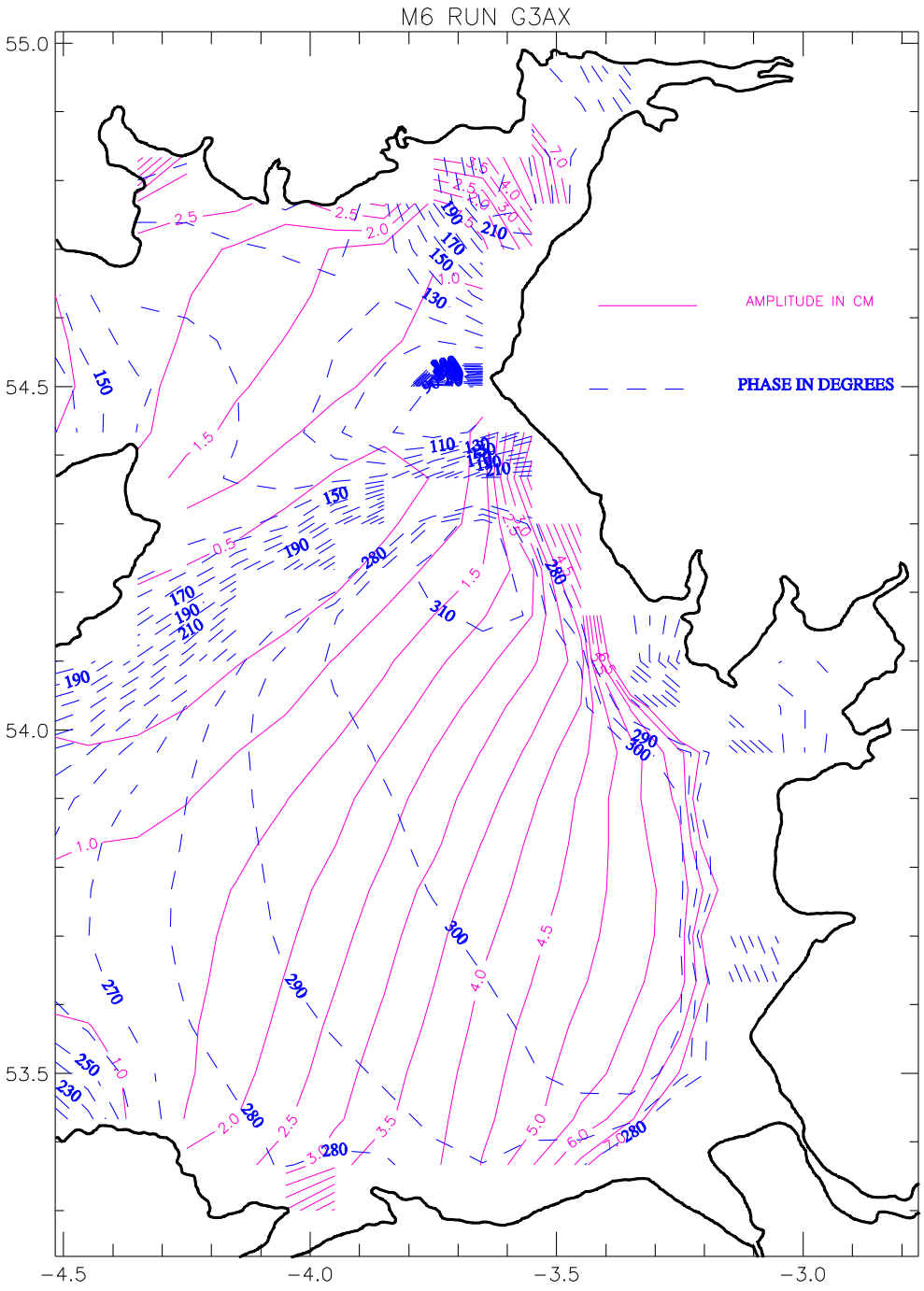
M6 RUN G3AX
AMPLITUDE IN CM
PHASE IN DEGREES
55.0
54.5
54.0
53.5
−4.5
−4.0
−3.5
−3.0

Fig3.3c(ii)

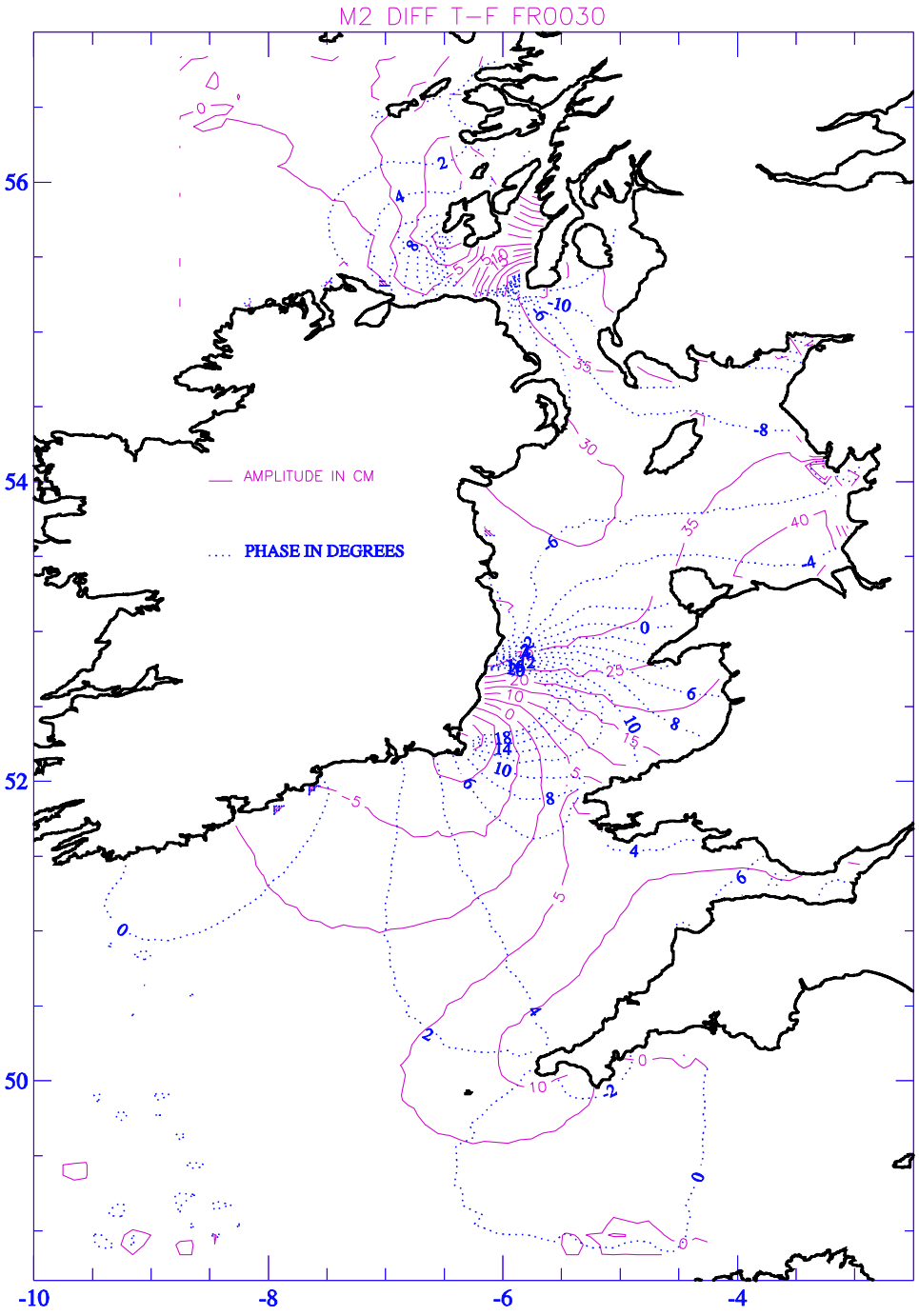
M2 DIFF T-F FR0030
AMPLITUDE IN CM
PHASE IN DEGREES
56
54
52
50
-10
-8
-6
-4

Fig. 4a(i)

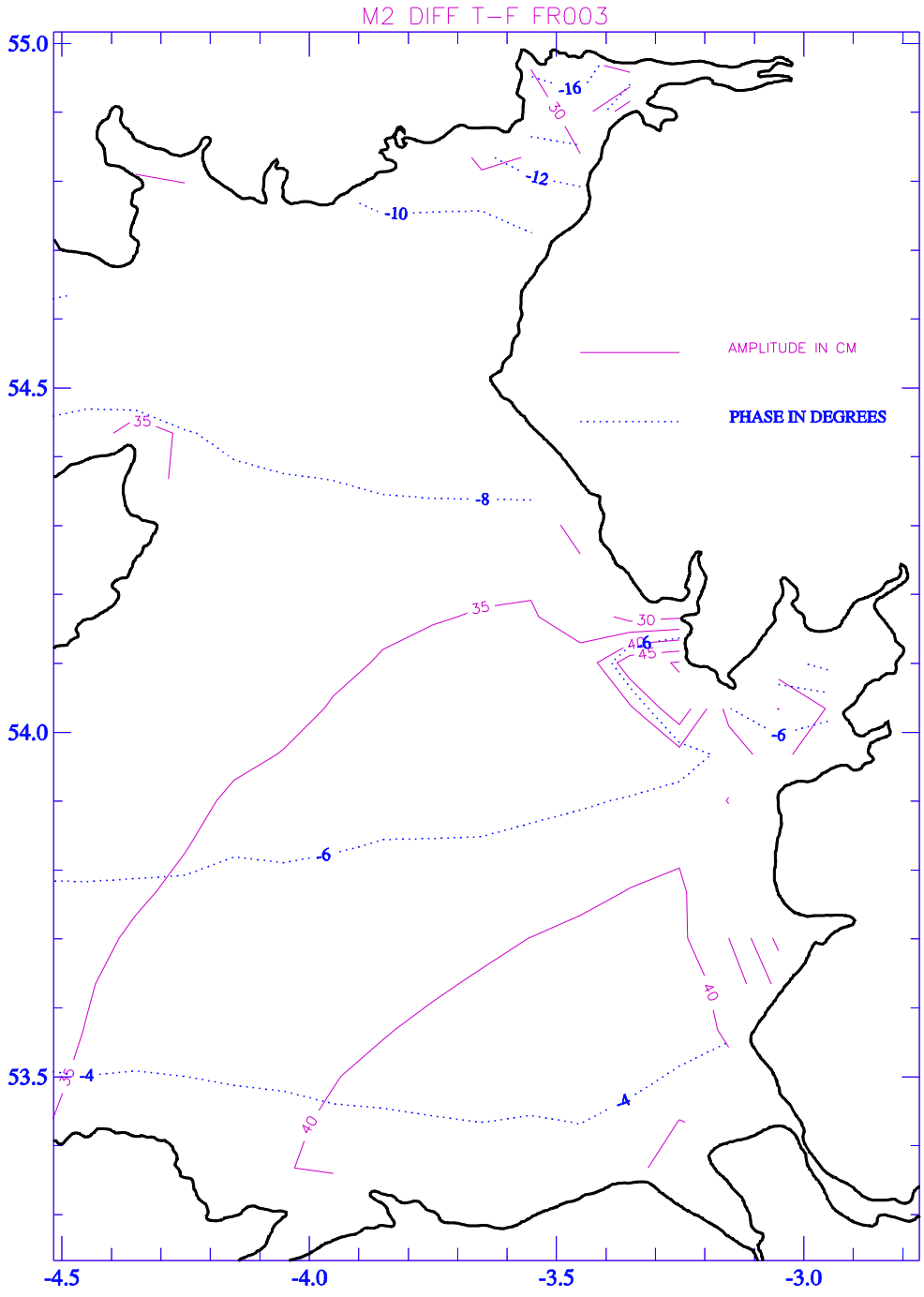
M2 DIFF T-F FR003
55.0
54.5
54.0
53.5
-4.5
-4.0
-3.5
-3.0
AMPLITUDE IN CM
PHASE IN DEGREES
-16
-12
-10
-8
-6
-4
35
30
40
45

Fig. 4a(ii)

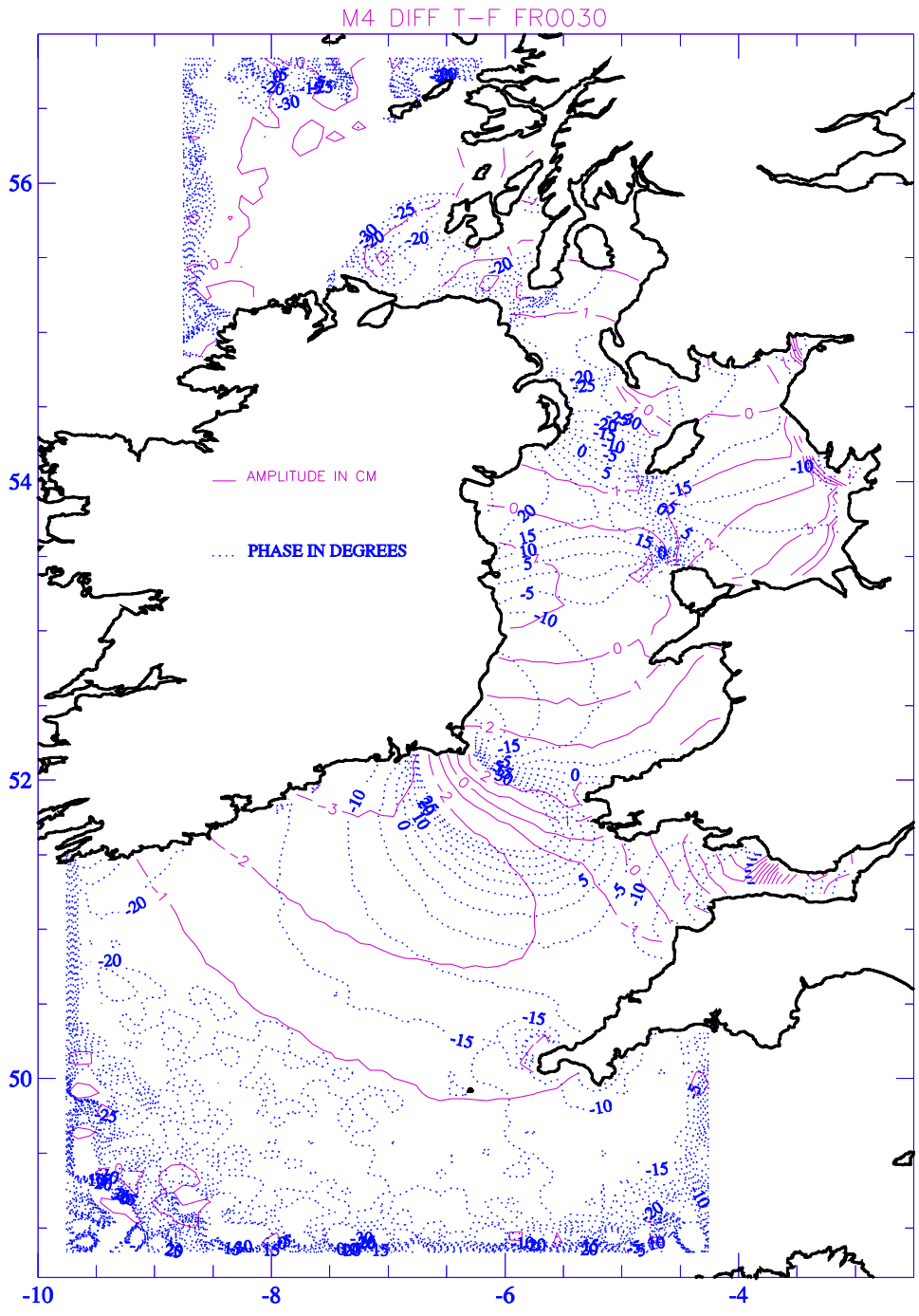
M4 DIFF T-F FR0030
AMPLITUDE IN CM
PHASE IN DEGREES
56
54
52
50
-10
-8
-6
-4

Fig. 4b(i)

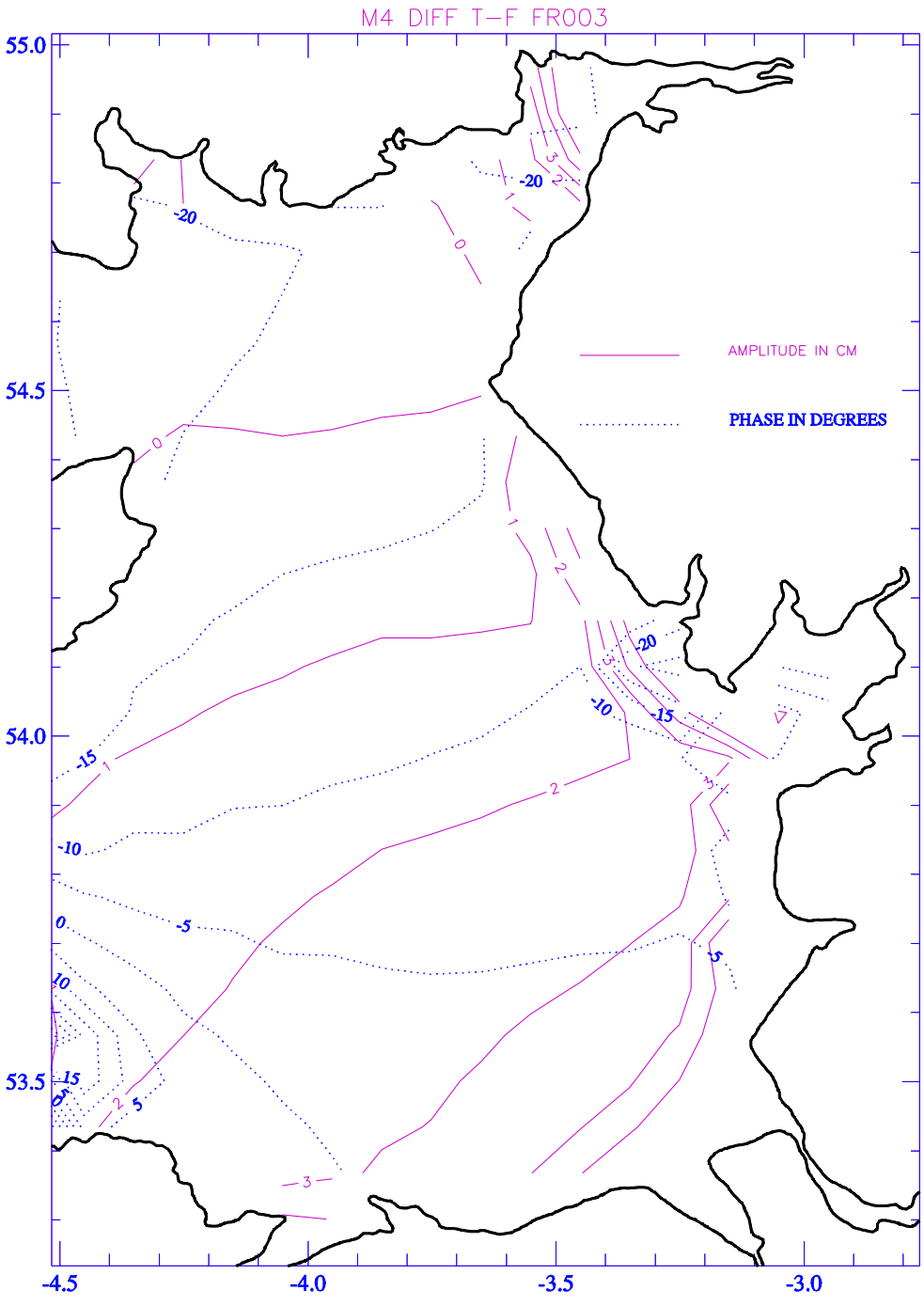
M4 DIFF T–F FR003
55.0
54.5
54.0
53.5
-4.5
-4.0
-3.5
-3.0
AMPLITUDE IN CM
PHASE IN DEGREES

Fig. 4b(ii)

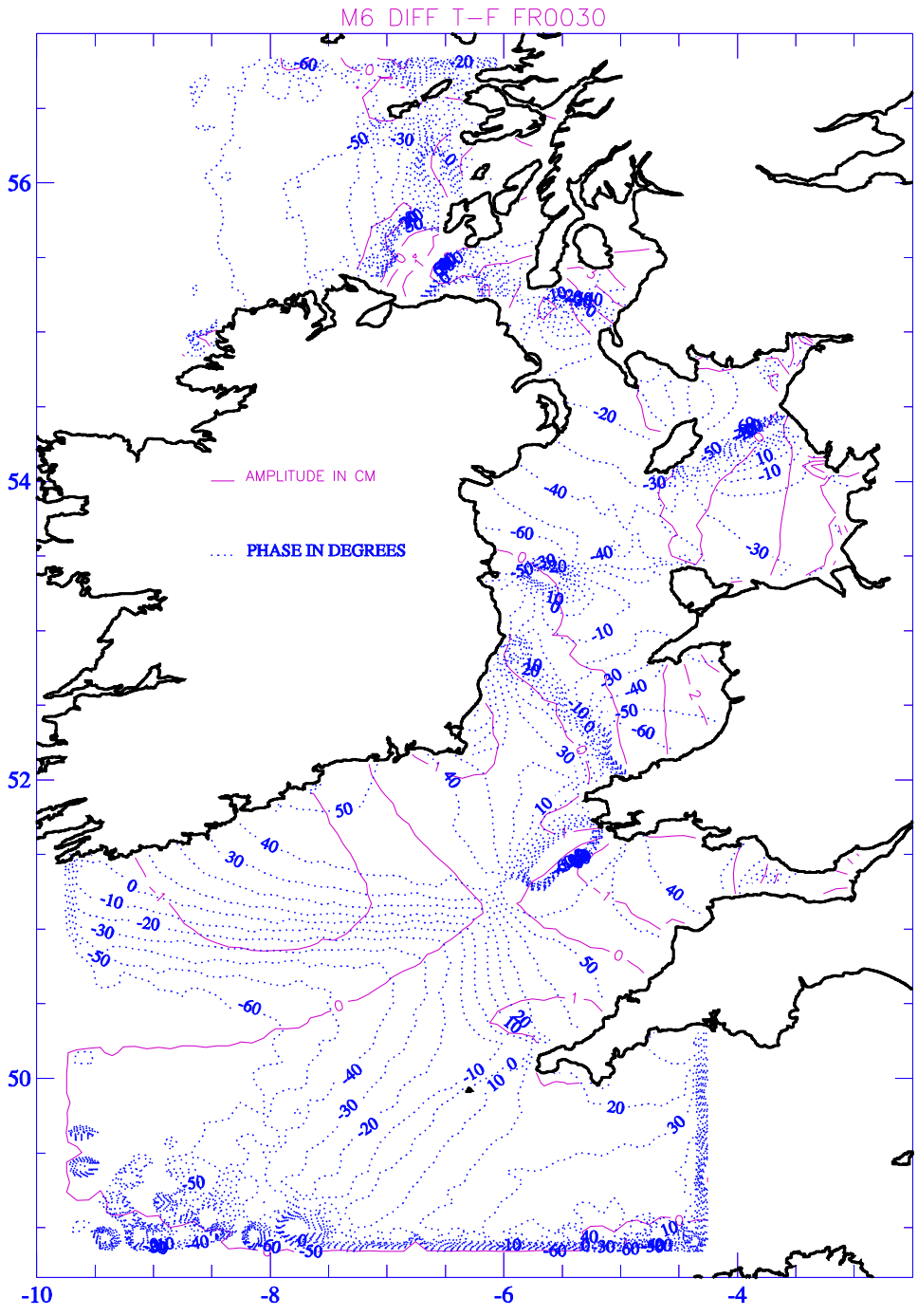
M6 DIFF T-F FR0030
AMPLITUDE IN CM
PHASE IN DEGREES
56
54
52
50
-10
-8
-6
-4

Fig. 4c(i)

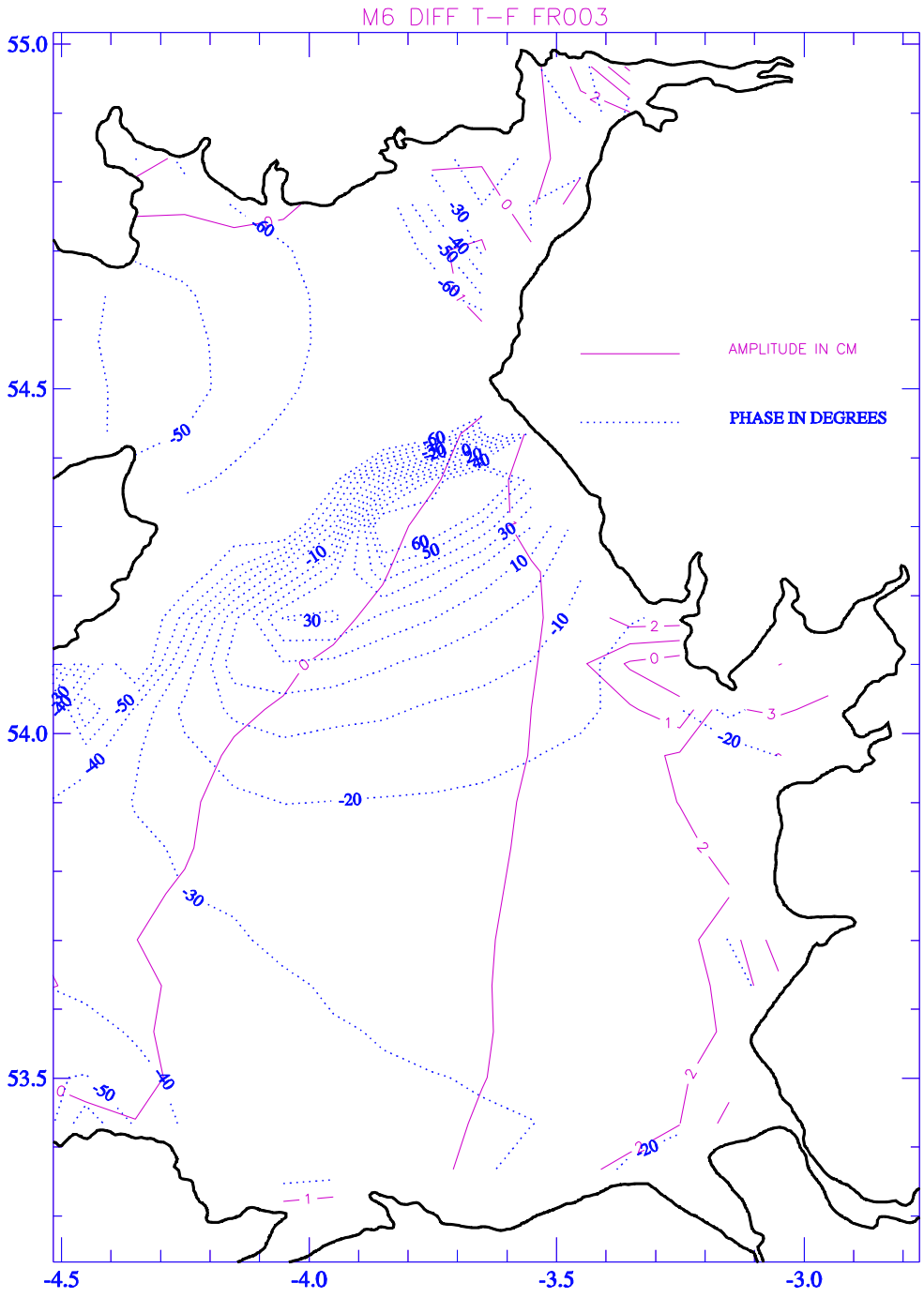
M6 DIFF T-F FR003
55.0
54.5
54.0
53.5
-4.5
-4.0
-3.5
-3.0
AMPLITUDE IN CM
PHASE IN DEGREES

Fig. 4c(ii)

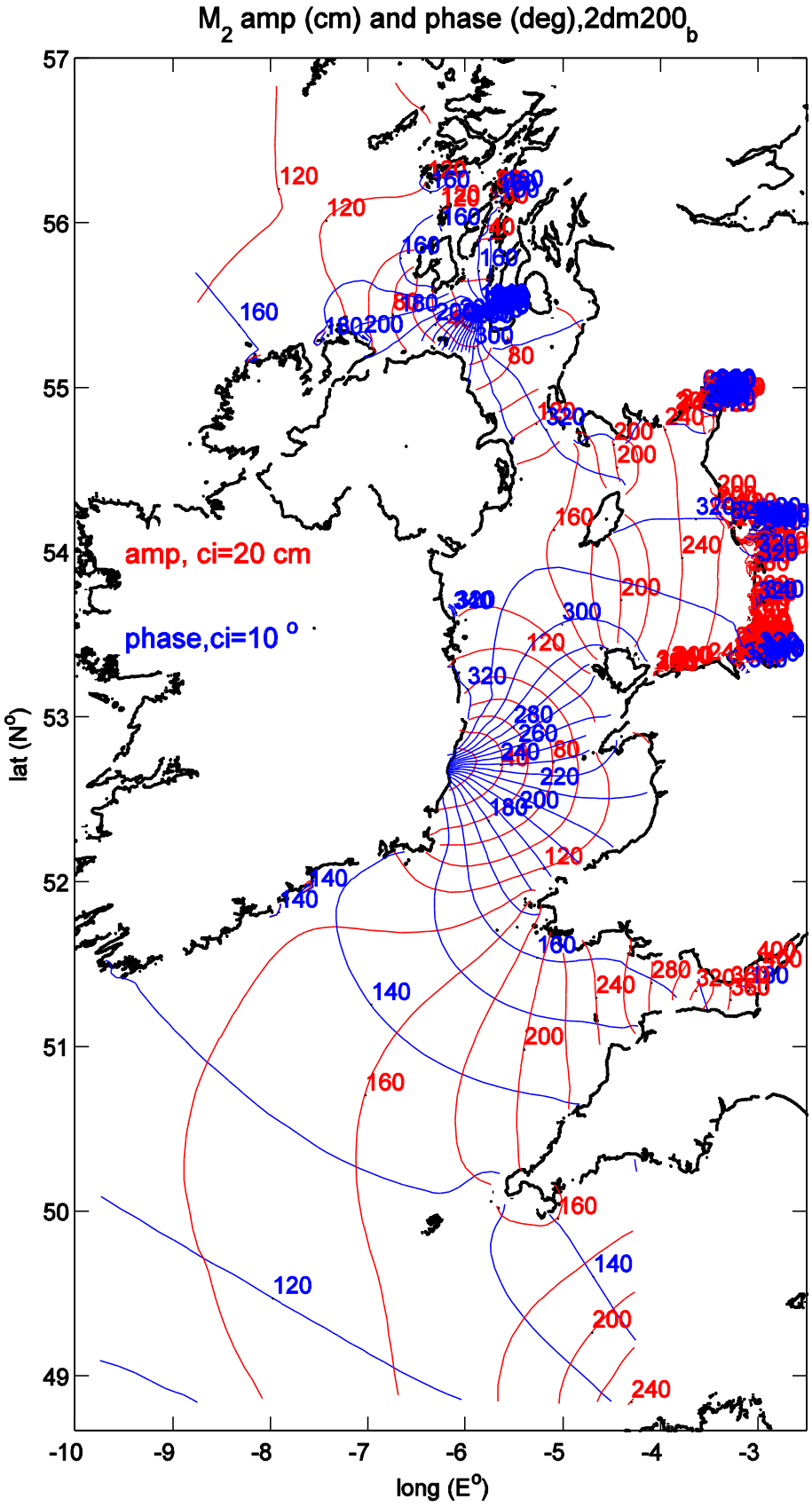

Fig. 5a(i)

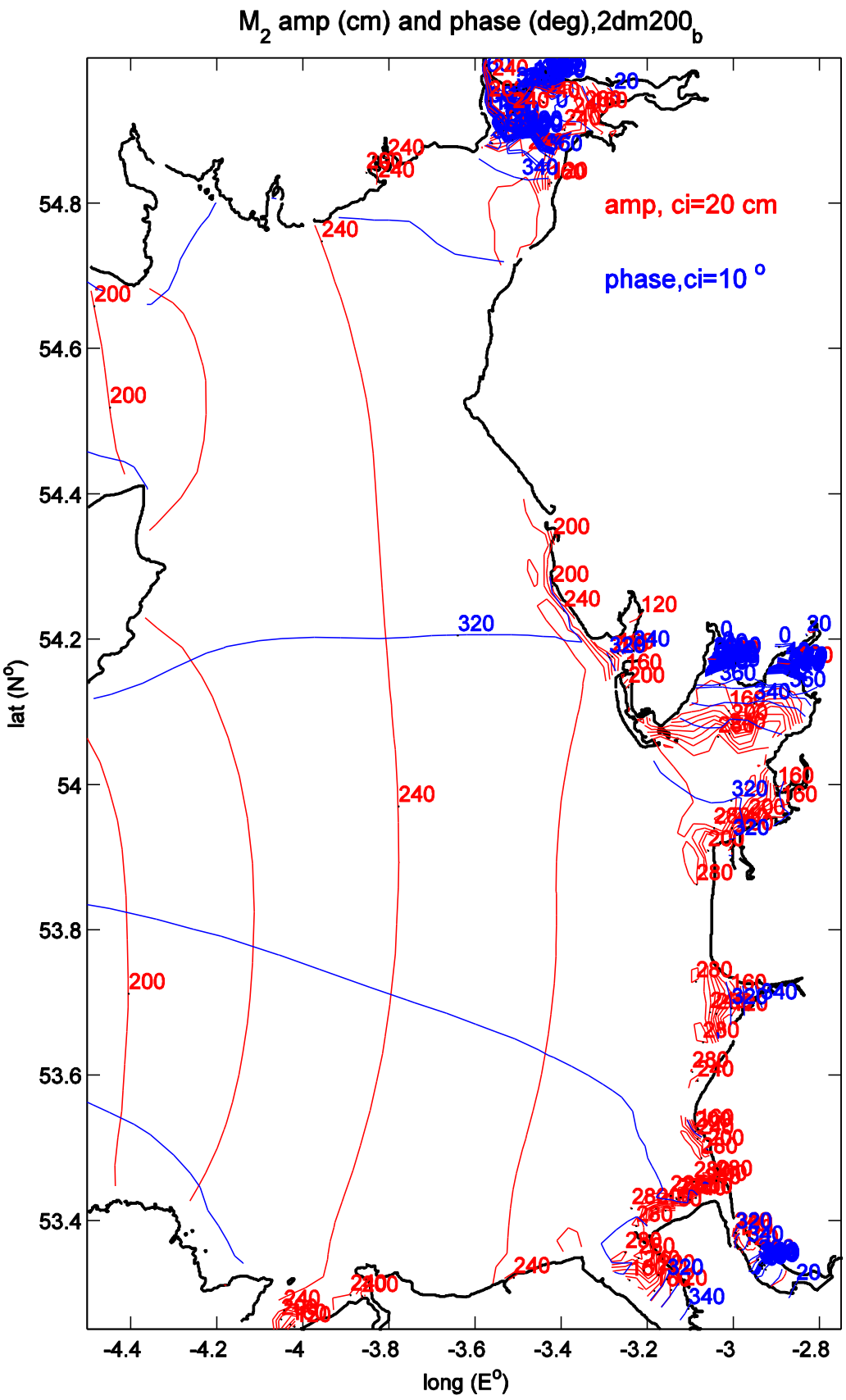
M2 amp (cm) and phase (deg),2dm200b
amp, ci=20 cm
phase,ci=10 °
lat (N°)
long (E°)
54.8
54.6
54.4
54.2
54
53.8
53.6
53.4
-4.4
-4.2
-4
-3.8
-3.6
-3.4
-3.2
-3
-2.8

Fig. 5a(ii)

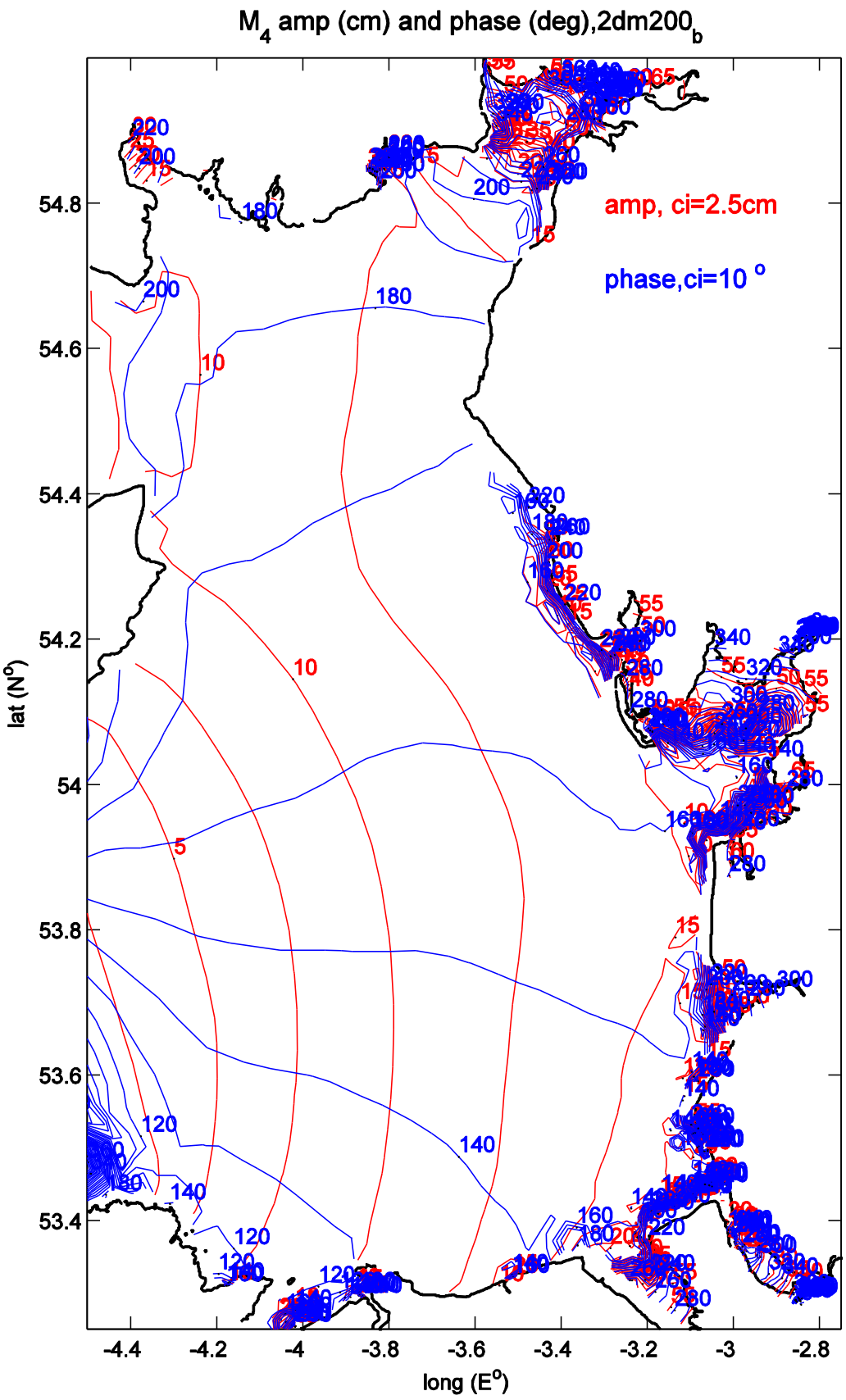
M4 amp (cm) and phase (deg),2dm200b
amp, ci=2.5cm
phase,ci=10 °
lat (N°)
long (E°)
54.8
54.6
54.4
54.2
54
53.8
53.6
53.4
-4.4
-4.2
-4
-3.8
-3.6
-3.4
-3.2
-3
-2.8

Fig. 5b

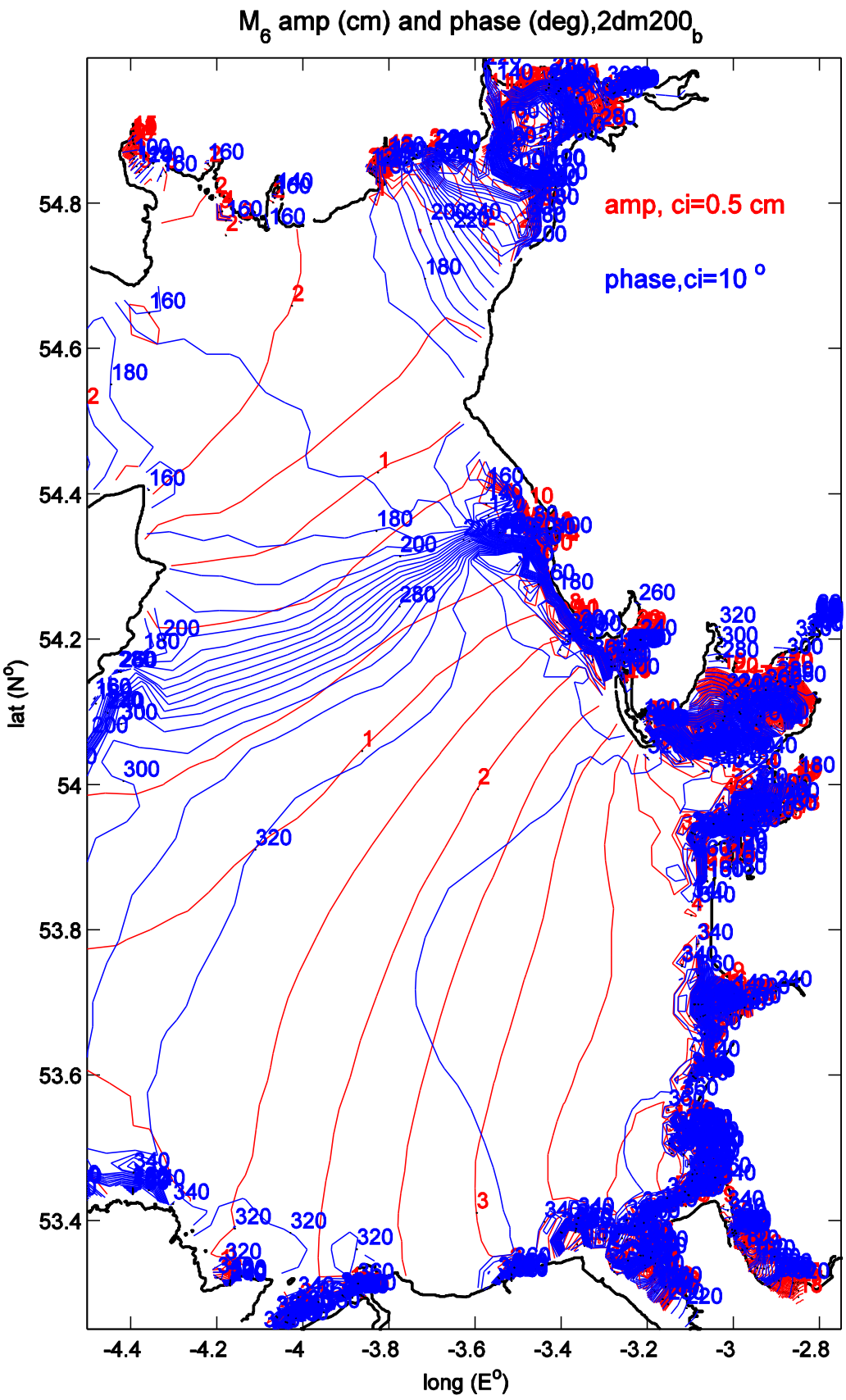
M6 amp (cm) and phase (deg),2dm200b
amp, ci=0.5 cm
phase,ci=10 °
lat (N°)
long (E°)
54.8
54.6
54.4
54.2
54
53.8
53.6
53.4
-4.4
-4.2
-4
-3.8
-3.6
-3.4
-3.2
-3
-2.8

Fi. 5c

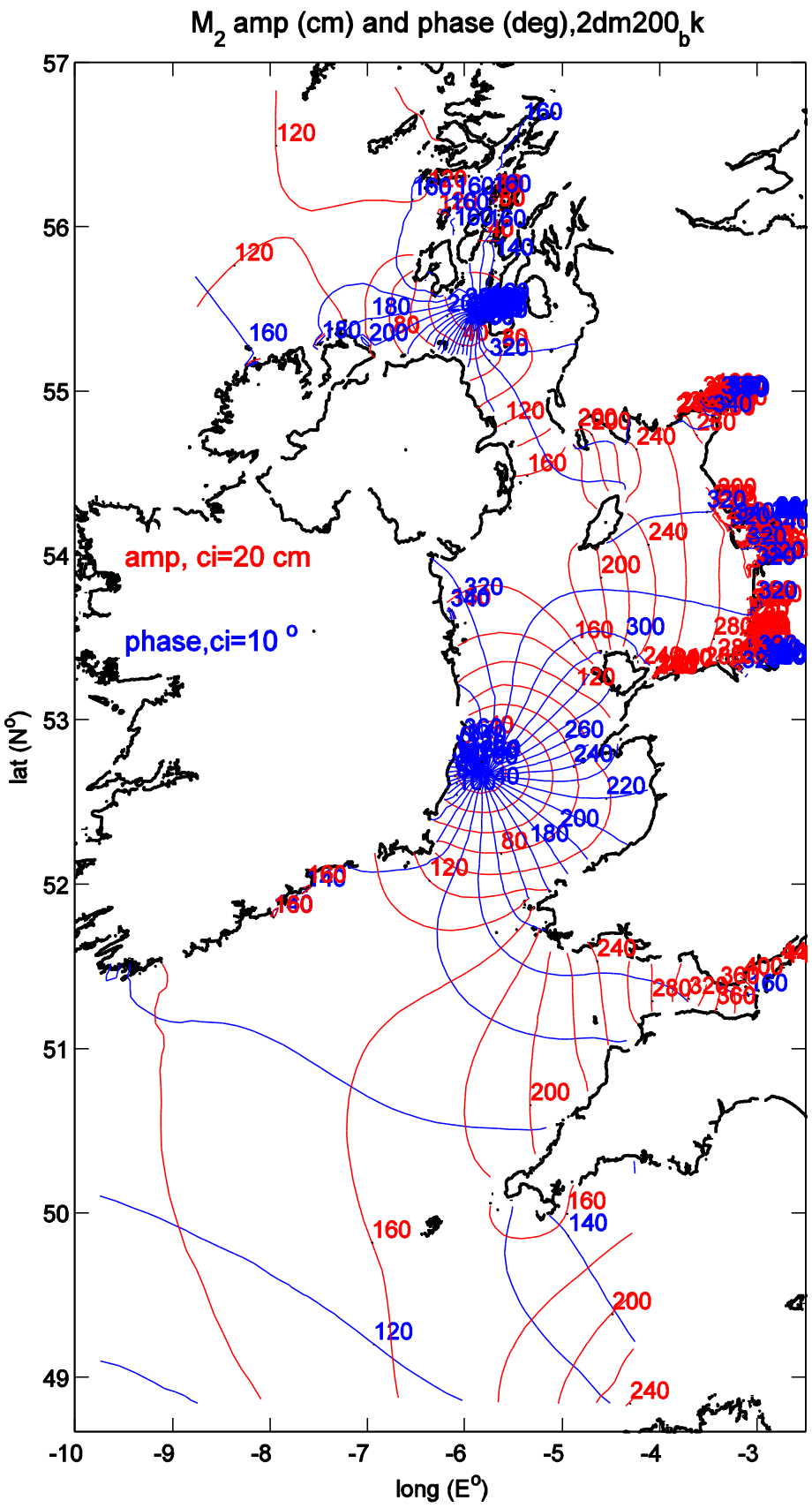
M2 amp (cm) and phase (deg),2dm200bk
amp, ci=20 cm
phase,ci=10 o
lat (No)
long (Eo)
57
56
55
54
53
52
51
50
49
-10
-9
-8
-7
-6
-5
-4
-3

Fig. 6a(i)

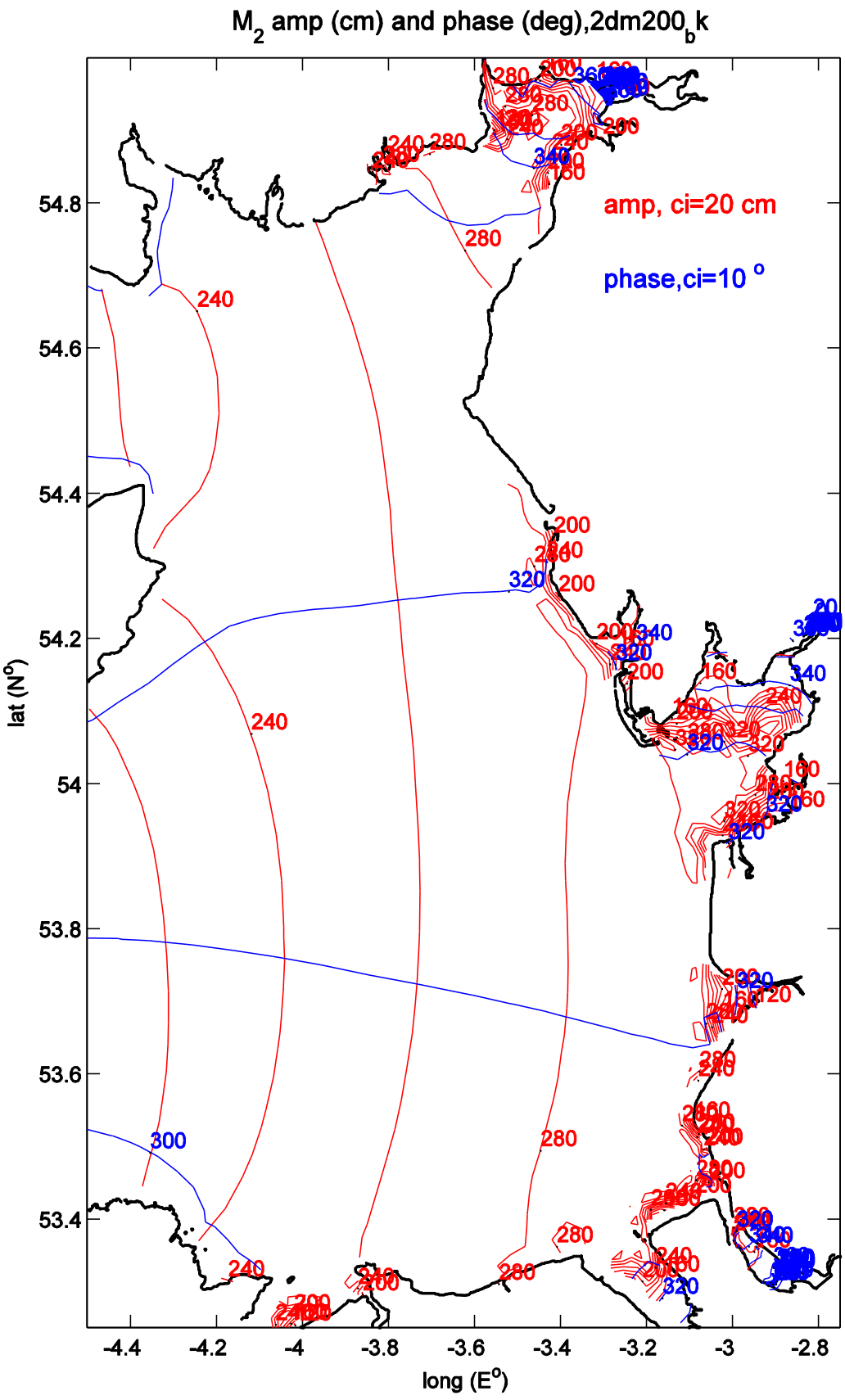
M2 amp (cm) and phase (deg),2dm200bk
amp, ci=20 cm
phase,ci=10 o
lat (No)
long (Eo)
54.8
54.6
54.4
54.2
54
53.8
53.6
53.4
-4.4
-4.2
-4
-3.8
-3.6
-3.4
-3.2
-3
-2.8

Fig. 6a(ii)

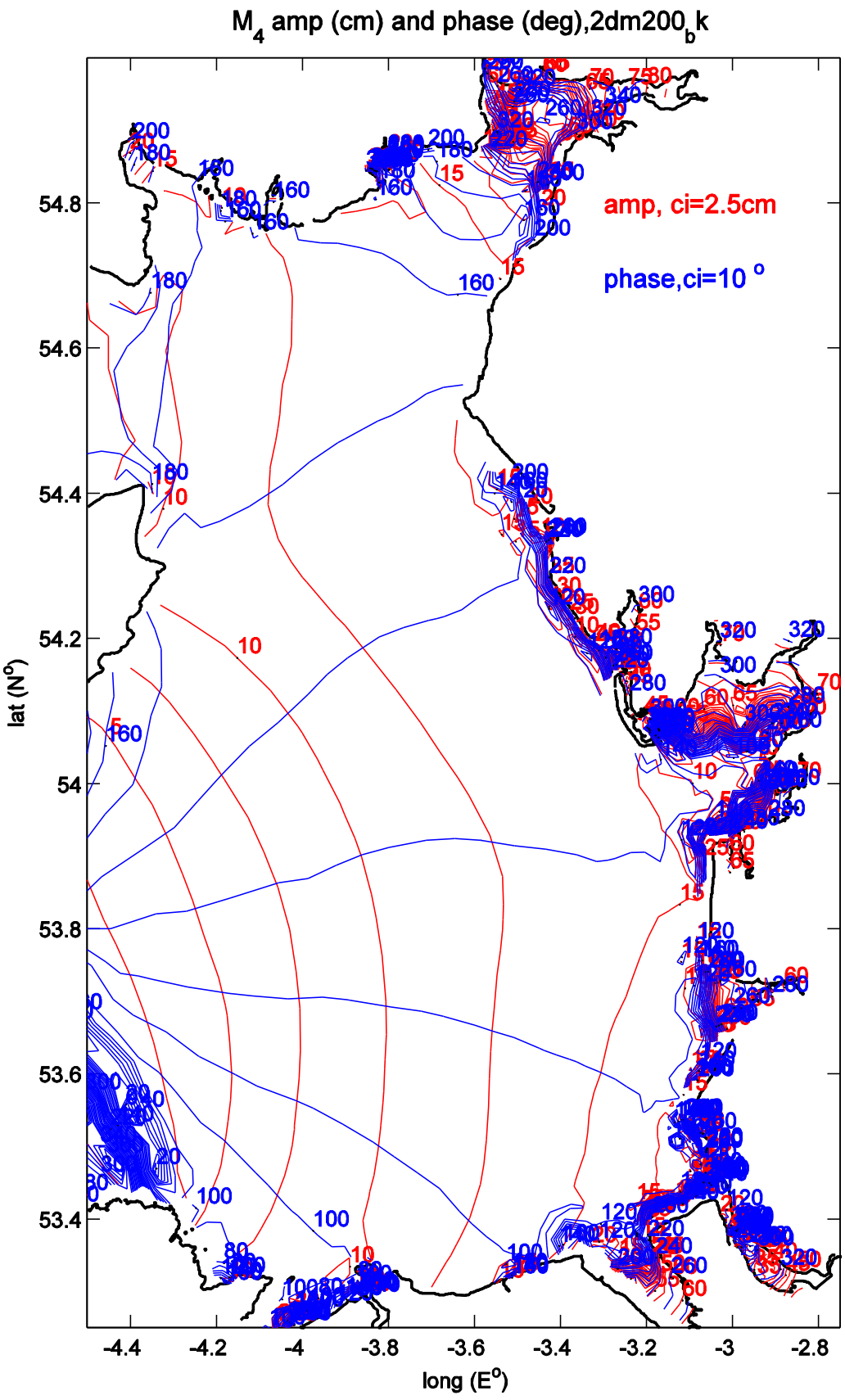
M4 amp (cm) and phase (deg),2dm200bk
amp, ci=2.5cm
phase,ci=10 °
lat (N°)
long (E°)
54.8
54.6
54.4
54.2
54
53.8
53.6
53.4
-4.4
-4.2
-4
-3.8
-3.6
-3.4
-3.2
-3
-2.8

Fig. 6b

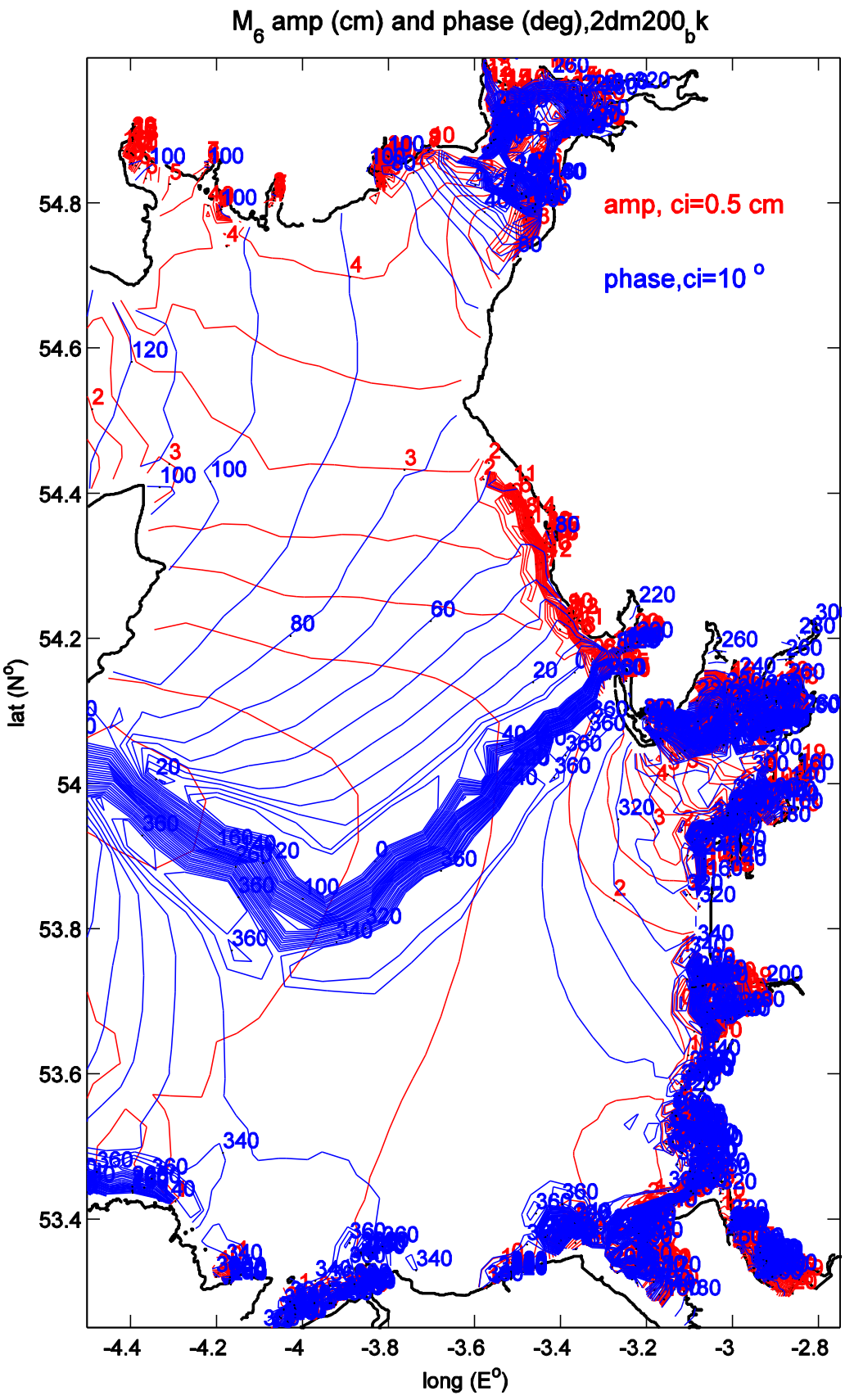
M6 amp (cm) and phase (deg),2dm200bk
amp, ci=0.5 cm
phase,ci=10 °
lat (N°)
long (E°)
54.8
54.6
54.4
54.2
54
53.8
53.6
53.4
-4.4
-4.2
-4
-3.8
-3.6
-3.4
-3.2
-3
-2.8

Fig. 6c

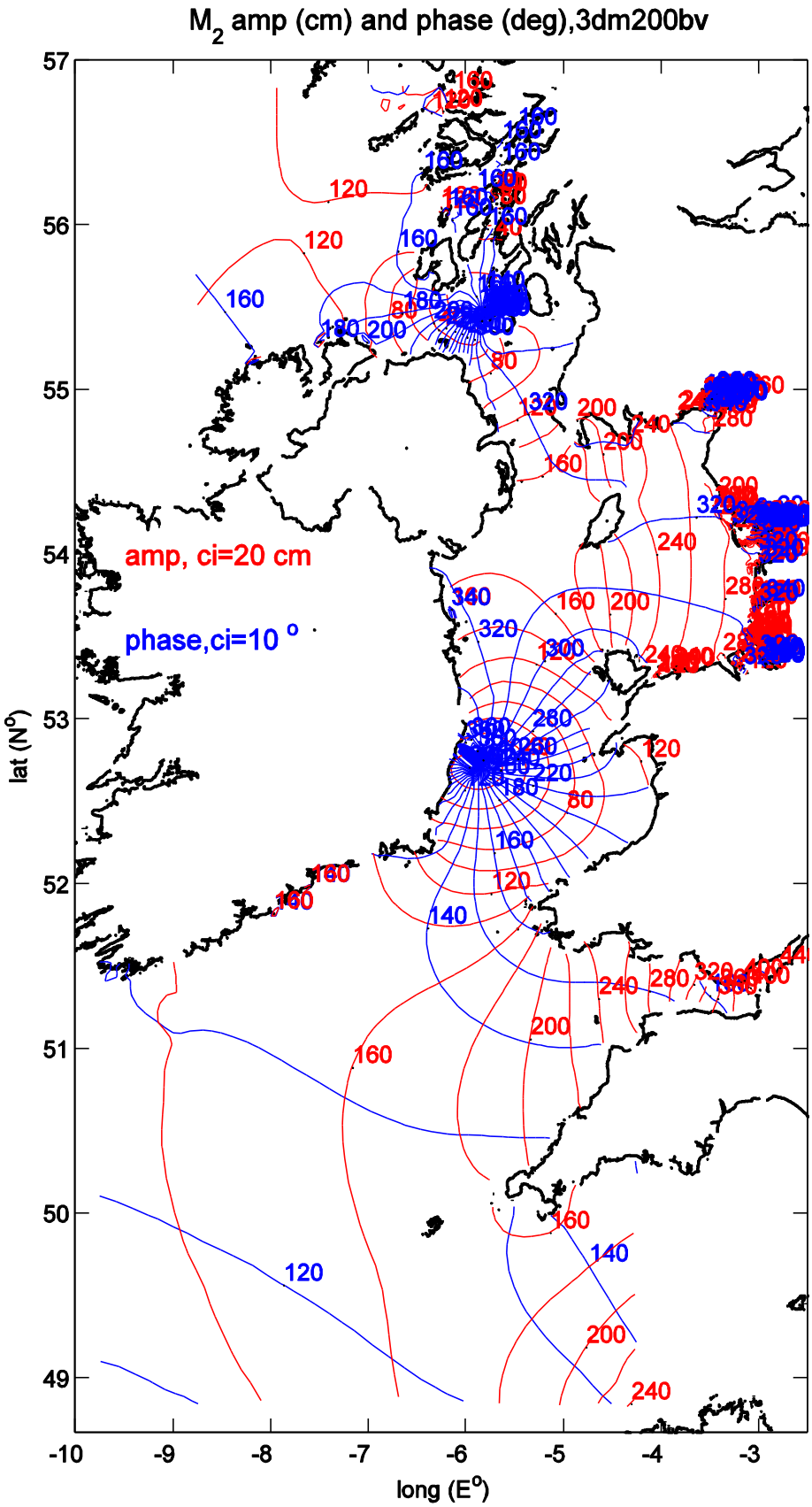
M2 amp (cm) and phase (deg),3dm200bv
amp, ci=20 cm
phase,ci=10 °
lat (N°)
long (E°)
57
56
55
54
53
52
51
50
49
-10
-9
-8
-7
-6
-5
-4
-3

Fig. 7a(i)

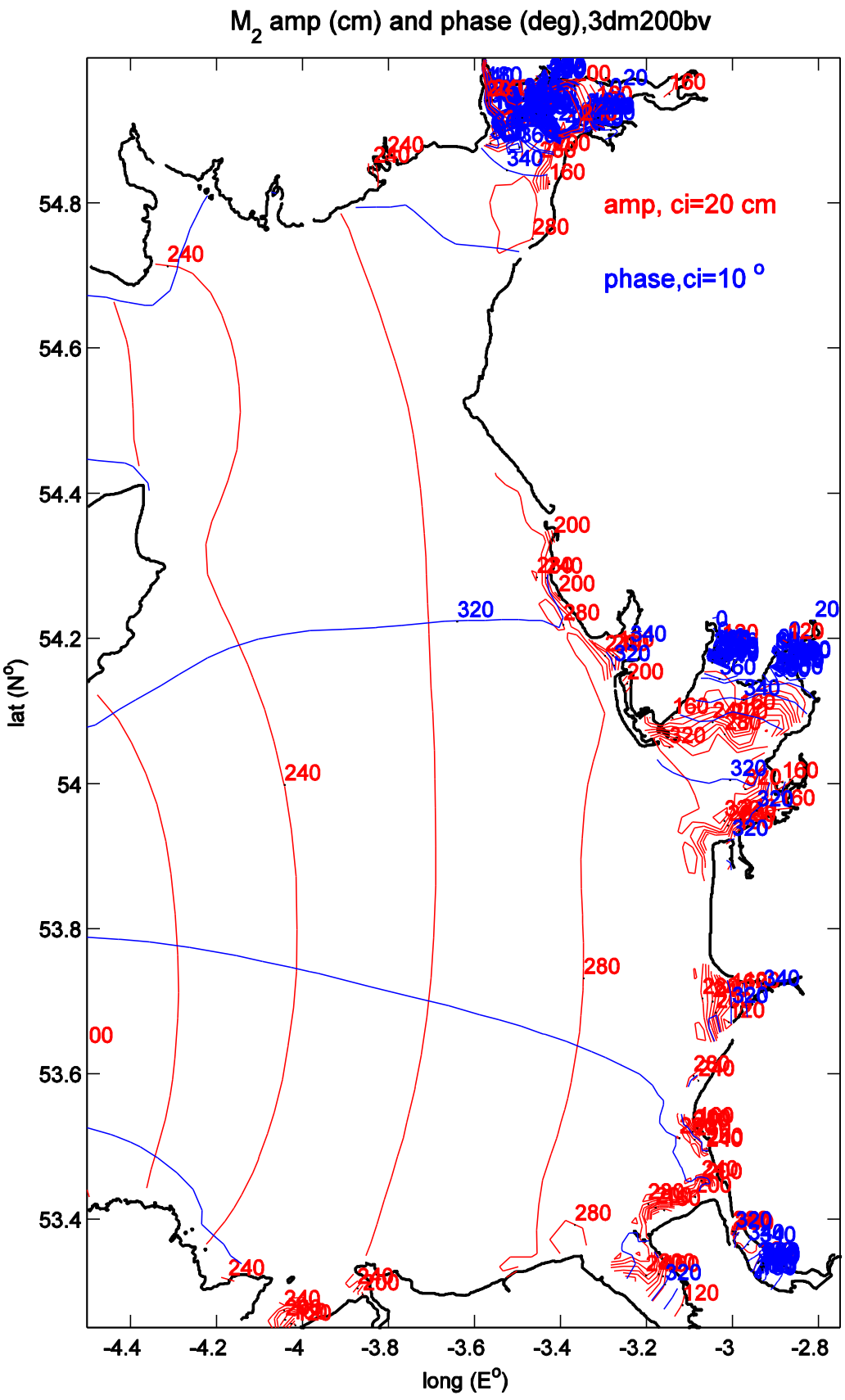
M2 amp (cm) and phase (deg),3dm200bv
amp, ci=20 cm
phase,ci=10 °
lat (N°)
long (E°)
54.8
54.6
54.4
54.2
54
53.8
53.6
53.4
-4.4
-4.2
-4
-3.8
-3.6
-3.4
-3.2
-3
-2.8

Fig. 7a(ii)

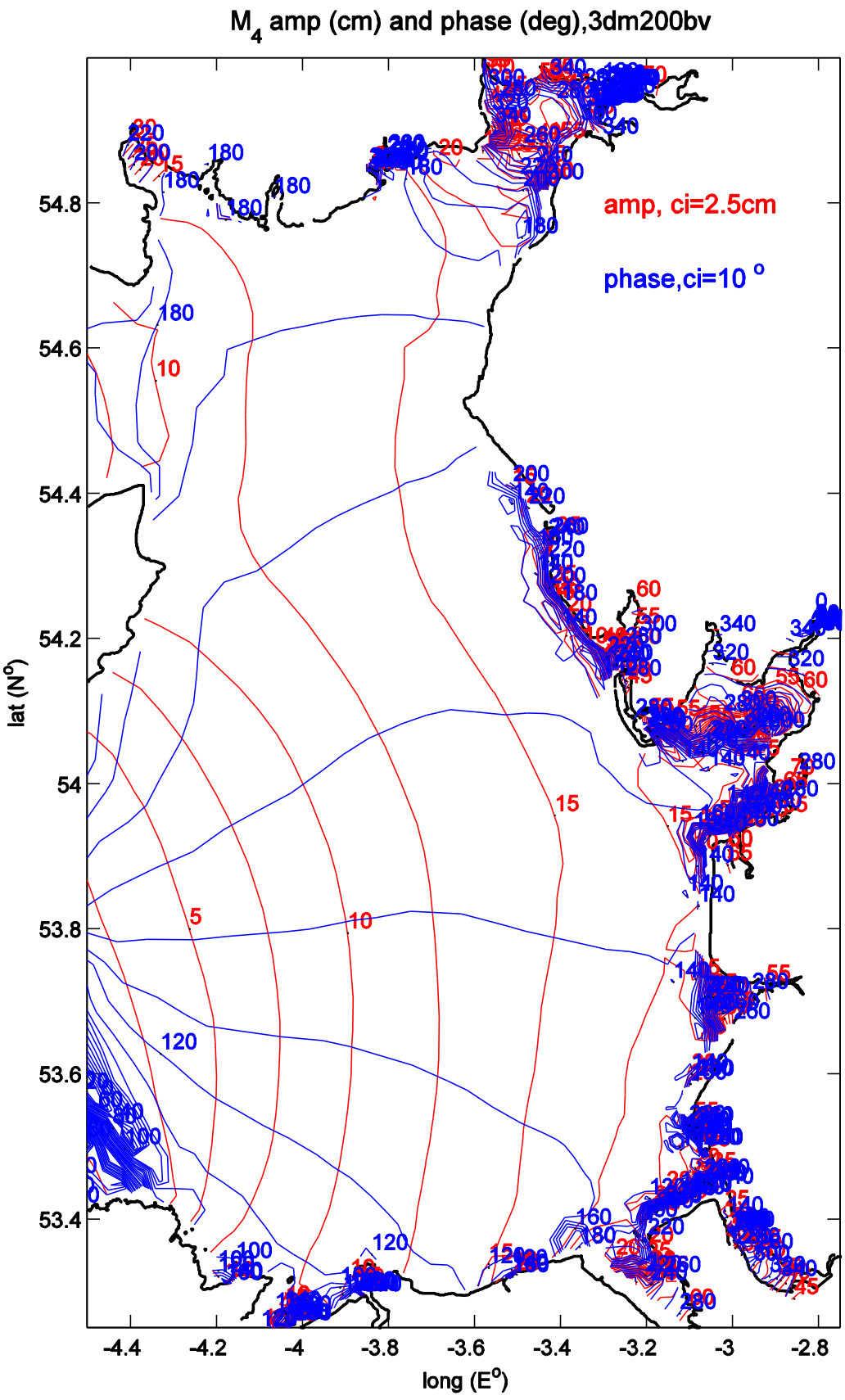
M4 amp (cm) and phase (deg),3dm200bv
amp, ci=2.5cm
phase,ci=10 °
lat (N°)
long (E°)
54.8
54.6
54.4
54.2
54
53.8
53.6
53.4
-4.4
-4.2
-4
-3.8
-3.6
-3.4
-3.2
-3
-2.8

Fig. 7b

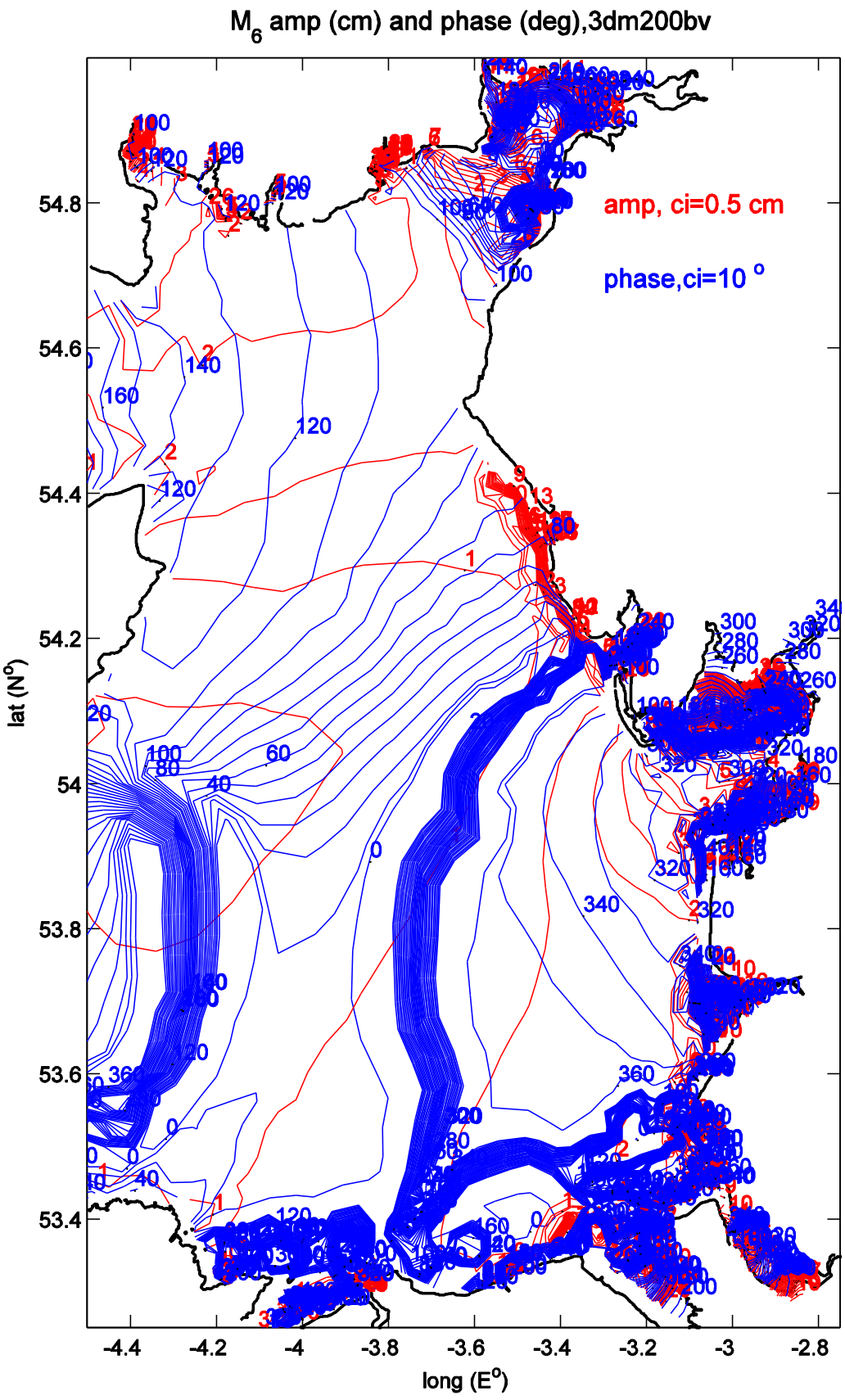
M6 amp (cm) and phase (deg),3dm200bv
amp, ci=0.5 cm
phase,ci=10 °
lat (N°)
long (E°)
54.8
54.6
54.4
54.2
54
53.8
53.6
53.4
-4.4
-4.2
-4
-3.8
-3.6
-3.4
-3.2
-3
-2.8

Fig. 7c